Charged particle timing at sub-25 picosecond precision: The PICOSEC detector

Ioannis Manthos

on behalf of the RD51 PICOSEC-Micromegas Collaboration

i.manthos@bham.ac.uk

Particle physics seminars @ University of Liverpool

17 March 2021

Timing with a few 10's of picosecond

- Needs for Precise timing bring us to the **picosec domain**
- E.g., in the **High Luminosity LHC**, 140-200 "pile-up" proton-proton interactions ("vertices") with happen in the same LHC clock, in close space (Gaussian +- 45mm).
- Using precise timing can separate particles coming from the various vertices.
- (3D) tracking of charged particles is not enough to associate them to the correct vertex . Including precise time offers an extra dimension of separation to achieve this.
- Requirement: **~30ps**

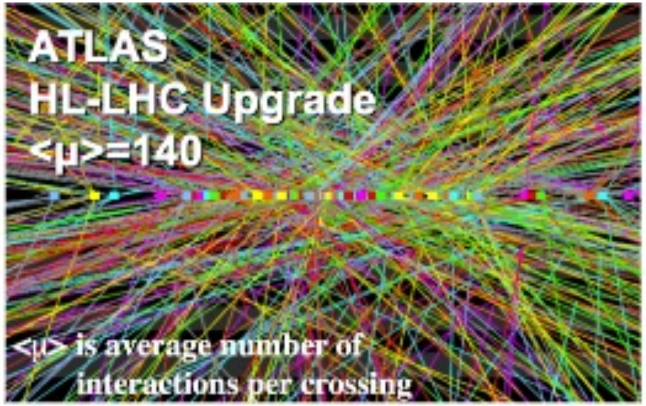

The association of the time measurement to the energy measurement is crucial for physics analysis, and requires time resolution of 20-30ps.

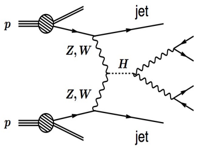

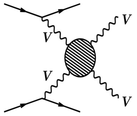

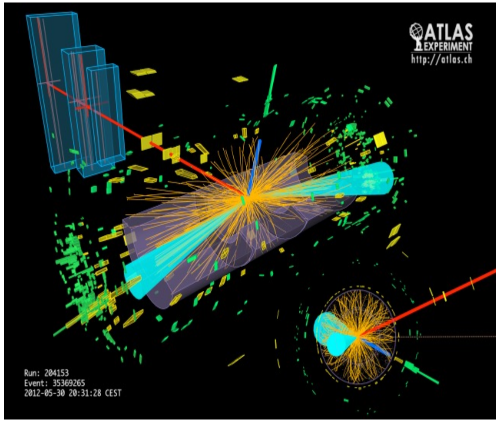

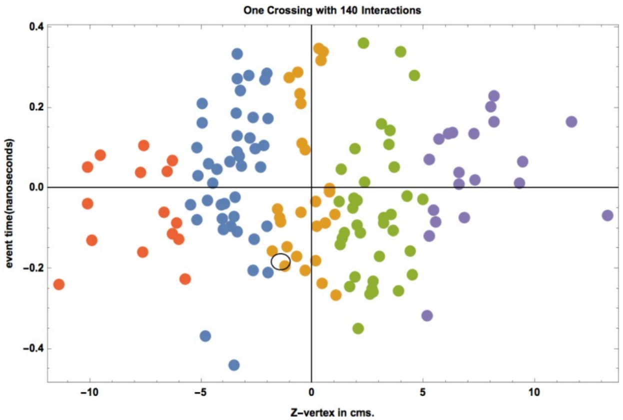

Existing Instrumentation:
e.g. Multi-Channel Plate (MCP) with **σ_t~ 4ps** but very expensive for large area coverage

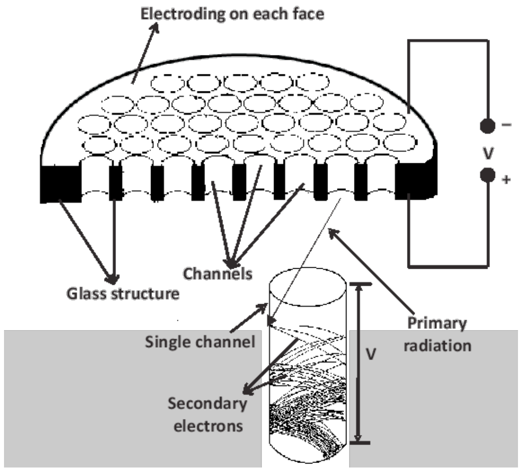

PhotoMultiplier: σ_t >800ps

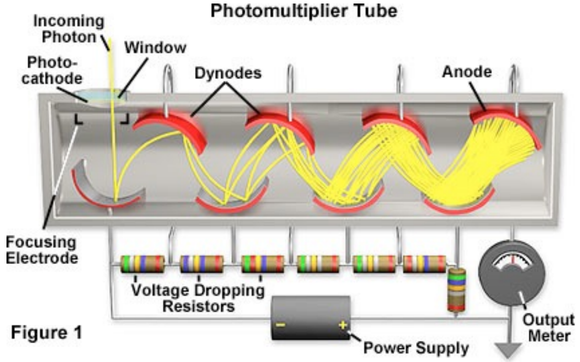

LHC experiments require large area coverage
MicroPattern Gas and **Silicon** structures candidate detector technologies.

To achieve time resolution for pileup mitigation to the order of 20-30 ps, both technologies require **significant modification** to reach the desired performance.

Large area detectors, resistant to radiation damage, with ~10ps timing capabilities will find applications in many other domains, e.g.

- particle identification in Nuclear and Particle Physics experiments
- photon's energy/speed measurements and correlations for Cosmology
- optical tracking for charge particles
- 4D tracking in the future accelerators (e.g. FCC with a center energy of ~100TeV)

MicroMegas: Micro Pattern Gaseous Chambers

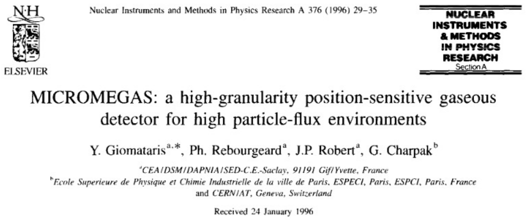

Nuclear Instruments and Methods in Physics Research A 376 (1996) 29–35

NUCLEAR INSTRUMENTS & METHODS IN PHYSICS RESEARCH Section A

ELSEVIER

MICROMEGAS: a high-granularity position-sensitive gaseous detector for high particle-flux environments

Y. Giomataris[a,*], Ph. Rebourgeard[a], J.P. Robert[a], G. Charpak[b]

[a]CEA/DSM/DAPNIA/SED-C.E.-Saclay, 91191 Gif/Yvette, France

[b]Ecole Superieure de Physique et Chimie Industrielle de la ville de Paris, ESPECI, Paris, ESPCI, Paris, France and CERN/AT, Geneva, Switzerland

Received 24 January 1996

https://doi.org/10.1016/0168-9002(96)00175-1

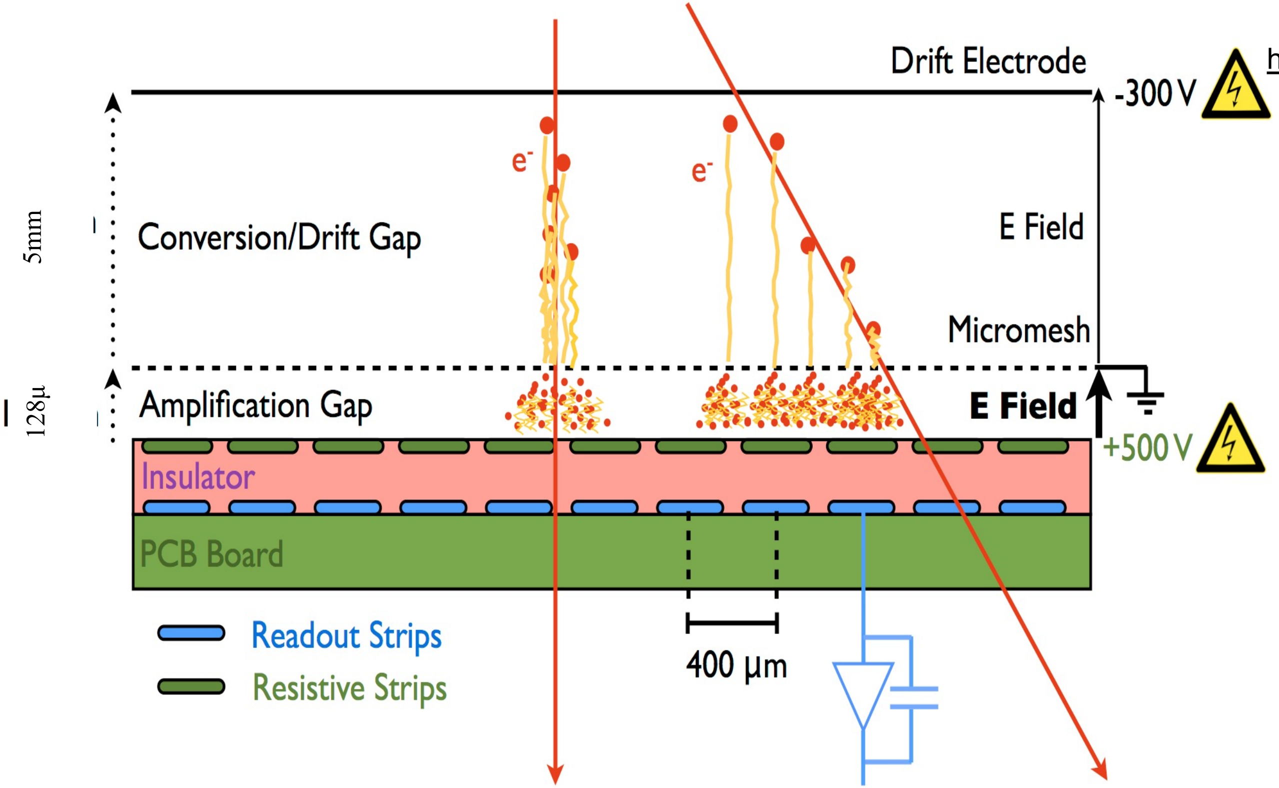

MicroMegas @ ATLAS experiment

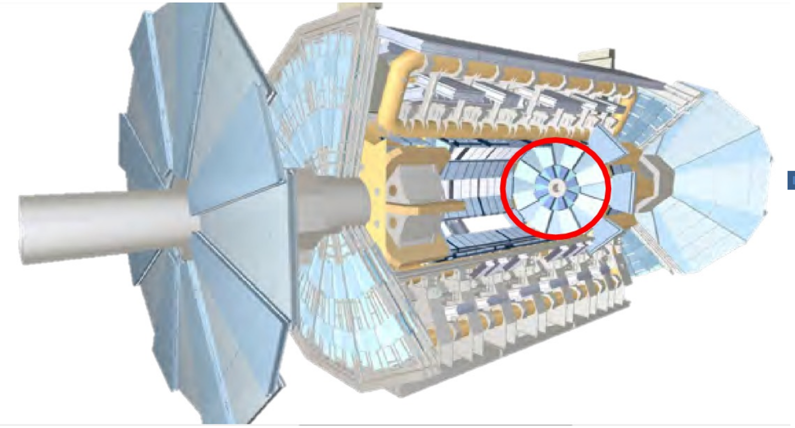

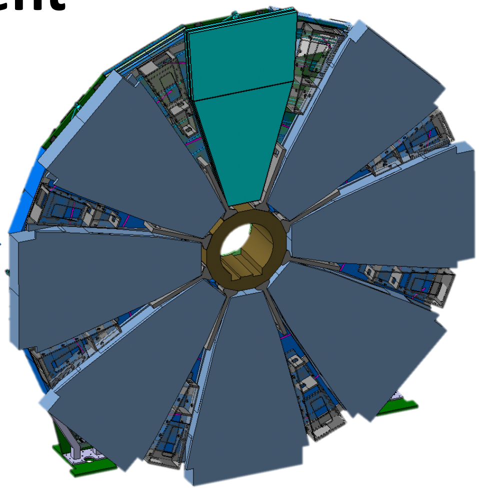

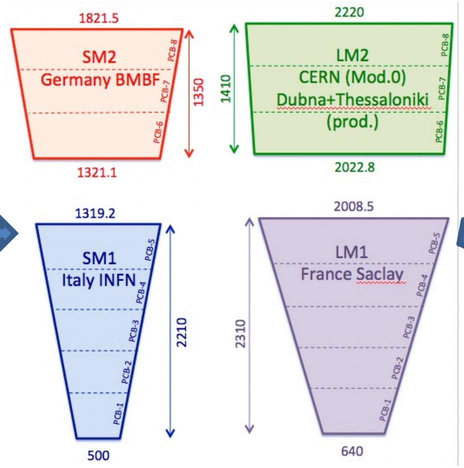

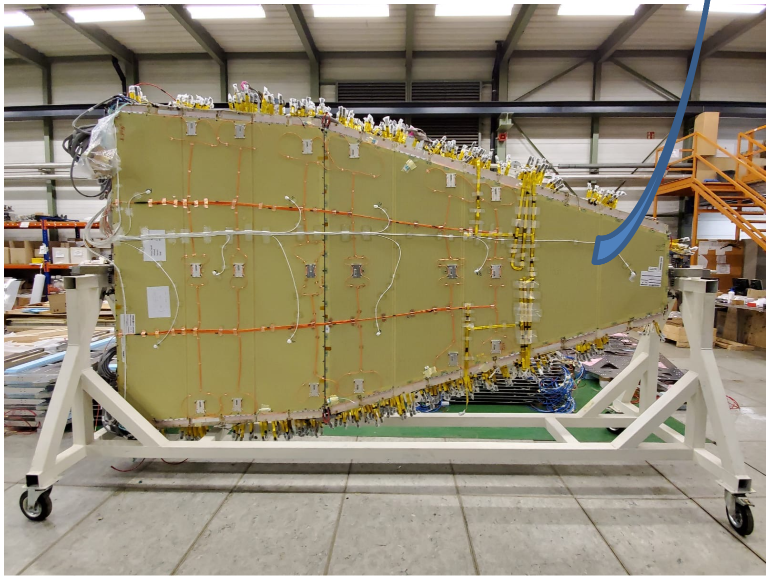

Large area coverage: 1200 m^2

- Momentum resolution: better than 15% up to p_t= 1 TeV
- Single plane resolution: 100µm, independent from track angle
- Track segment reconstruction: 50 µm
- Track segment efficiency: >= 97% @ p_t> 10 GeV
- Online angular resolution (trig): <= 1 mrad
- Spatial resolution 2nd coordinate: ~cm, from stereo strips or wires
- Hit rate capability: 15 kHz/cm^2 (meeting perform. requ.)
- Accumulated charge without ageing: 1 C/cm^2 (3000 fb^{-1} w/o degradation)

The Physics of Ionization offers the means for precise spatial measurements (high spatial resolution) but inhibits precise timing measurements

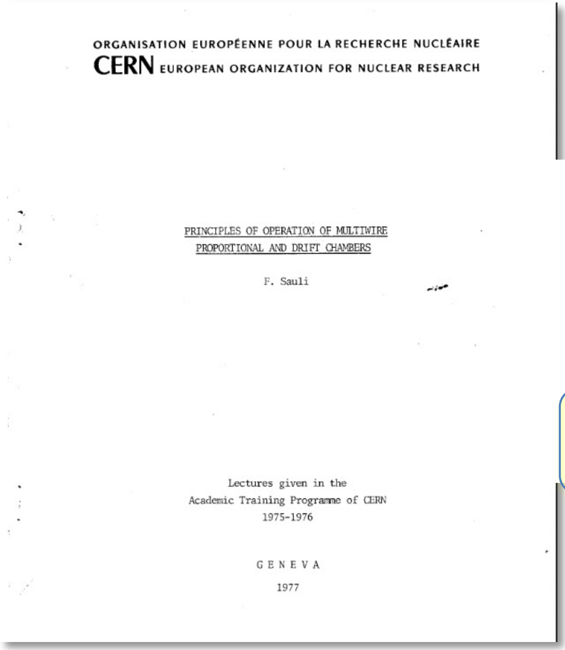
ORGANISATION EUROPÉENNE POUR LA RECHERCHE NUCLÉAIRE
CERN EUROPEAN ORGANIZATION FOR NUCLEAR RESEARCH

PRINCIPLES OF OPERATION OF MULTIWIRE PROPORTIONAL AND DRIFT CHAMBERS

F. Sauli

Lectures given in the Academic Training Programme of CERN 1975-1976

GENEVA
1977

10.5170/CERN-1977-009

which is represented in Fig. 8, for n = 34, as a function of the coordinate across a 10 mm thick detector. If the time of detection is the time of arrival of the closest electron at one end of the gap, as is often the case, the statistics of ion-pair production set an obvious limit to the time resolution of the detector. A scale of time is also given in the figure, for a collection velocity of 5 cm/μsec typical of many gases; the FWHM of the distribution is about 5 nsec. There is no hope of improving this time resolution in a gas counter, unless some averaging over the time of arrival of all electrons is realized.

In order to use gaseous detectors for precise (ps) timing of charged particles we should turn other Physics phenomena against the stochastic Nature of ionization

- Cherenkov radiation → provide prompt photons
- Photoelectric effect → convert photons to prompt electrons

1. PICOSEC MicroMegas: a detector with precise timing

Detector concept

RD51 PICOSEC-MicroMegas Collaboration

- **CEA Saclay (France):** S.Aune D. Desforge, I. Giomataris, T. Gustavsson, F.J. Iguaz[1], M. Kebbiri, P. Legou, O. Maillard, T. Papaevangelou, M. Pomorski,, L. Sohl
- **CERN (Switzerland):** J. Bortfeldt, F. Brunbauer, C. David,M. Lisowska, M. Lupberger, H. Müller, E. Oliveri, F. Resnati, L. Ropelewski, L. Scharenberg, T. Schneider, M. van Stenis, A. Utrobicic, R. Veenhof[2], S.White[3]
- **USTC (China):** J. Liu, B. Qi, X. Wang, Z. Zhang, Y. Zhou
- **AUTH (Greece):** K. Kordas, C. Lampoudis, I. Maniatis, I. Manthos[4], K. Paraschou, D. Sampsonidis, S.E. Tzamarias
- **NCSR (Greece):** G. Fanourakis
- **NTUA (Greece):** Y. Tsipolitis
- **LIP (Portugal):** M. Gallinaro
- **HIP (Finland):** F. García

1) Now at Synchrotron Soleil, 91192 Gif-sur-Yvette, Fran
2) Also MEPhI & Uludag University.
3) Also University of Virginia.
4) Now at University of Birmingham, UK

PICOSEC Micromegas

PICOSEC detector concept

- **Classic Micromegas**

  Giomataris Y. et al., NIMA 376(1996) 29

- Multiple electrons produced at different points along particle's path in the ~3-6mm drift region
  → <u>Time jitter order: **few ns**</u>

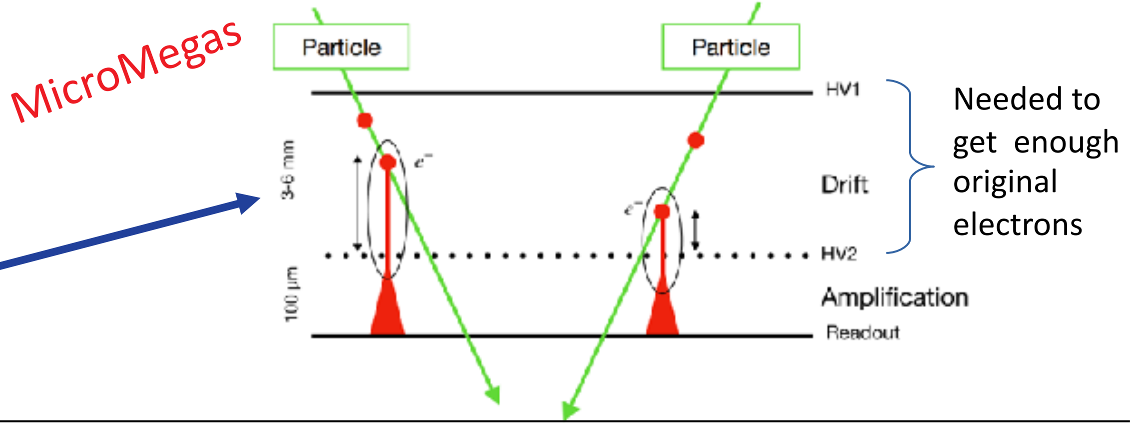

- **Micromegas + Cherenkov radiator + photocathode** → synchronous photo-electrons enter Micromegas

- **Small drift gap** & high field → avalanches start as early as possible with minimal time jitter → <u>Timing resolution a **few tens of ps**</u>

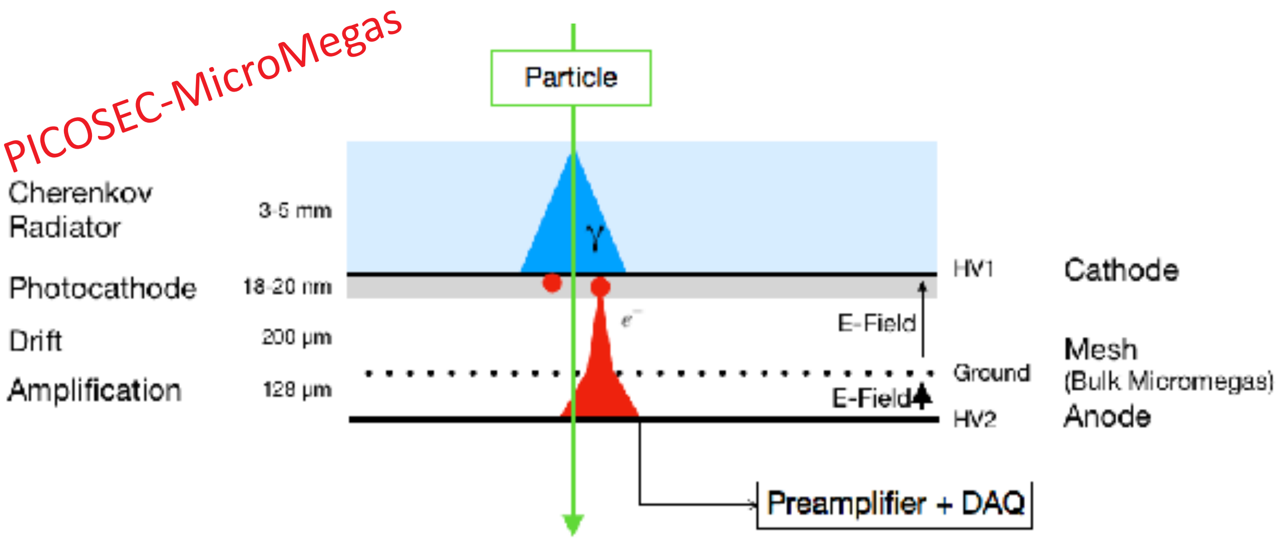

PICOSEC single-channel Prototype

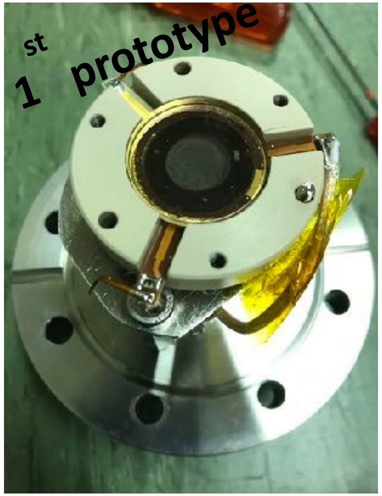

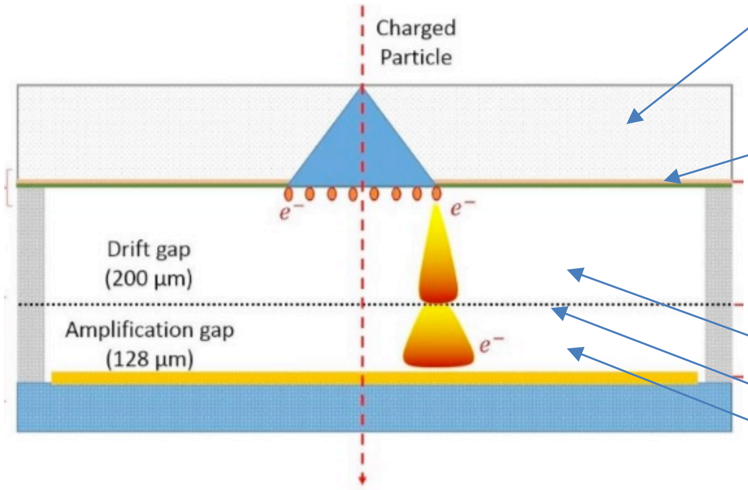

Single pad prototypes - 1 cm diameter active area

* Cherenkov Radiator:
MgF_2 3 mm thick → <u>3 mm Cherenkov cone</u>

* Photocathode: 18nm CsI (with 5.5 nm Cr - cathode)

* COMPASS gas (80% Ne + 10% CF_4 + 10% C_2H_6)
Pressure: 1 bar.

* Drift gap = 200 μm
* Mesh thickness = 36 μm (centered at 128 μm above anode)
* Amplification gap = 128 μm

- Bulk MicroMegas readout (6 pilars)
- 4 kapton rings spacers → 200 μm drift

Results from Laser and Beam tests presented next are from this detector
Since 2016, different prototypes studied (bulk, thin mesh etc. MM, multipad MM, different gas, anode schemes, photocathodes)

1. A precise-timing detector

proof with results of single-channel prototypes
Response to single photoelectrons

Laser beam: response to single electron

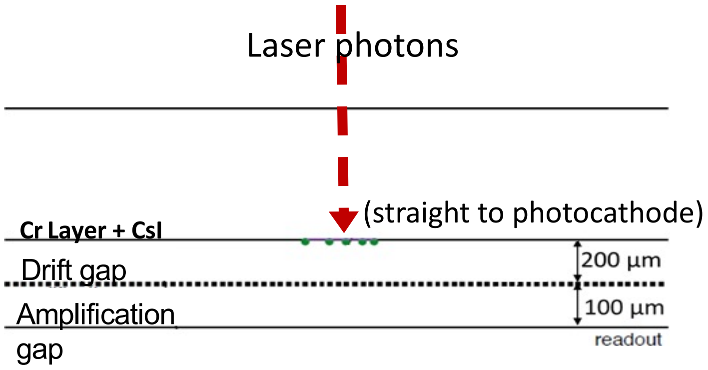

- **Pulsed laser** at IRAMIS facility (CEA Saclay)
- Wavelength: 267-288 nm
- Repetition rate: up to 500 kHz
- **Intensity: attenuated to get single photoelectron directly on photocathode**
- Read out with CIVIDEC preamp
- **Digitized waveform by 2.5GHz LeCroy oscilloscope @ 20GSamples/s = 1 sample/50ps.**
- t_0 reference: fast photodiode (~10 ps resolution)

Typical single p.e signal

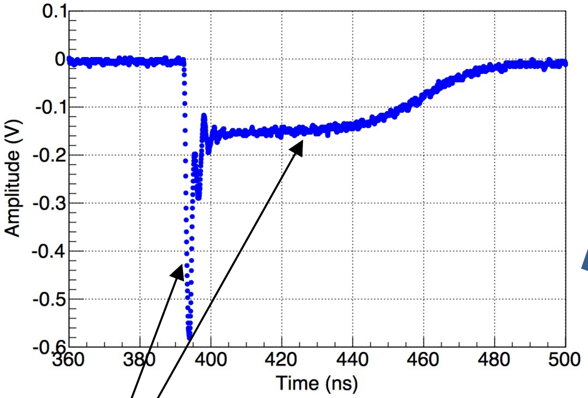

Signal inverted

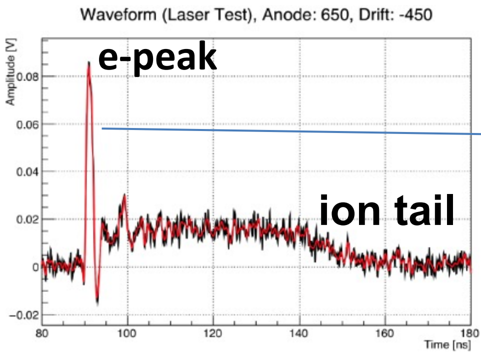

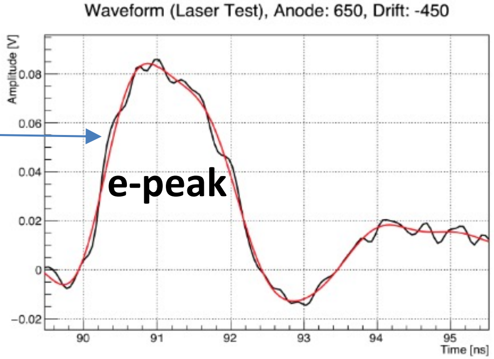

Two-component signal:

* **Electron peak** (“*e-peak*”) → fast (~0.5ns)

* **Ion tail** → slow (~100ns)

Signal processing: Timing method

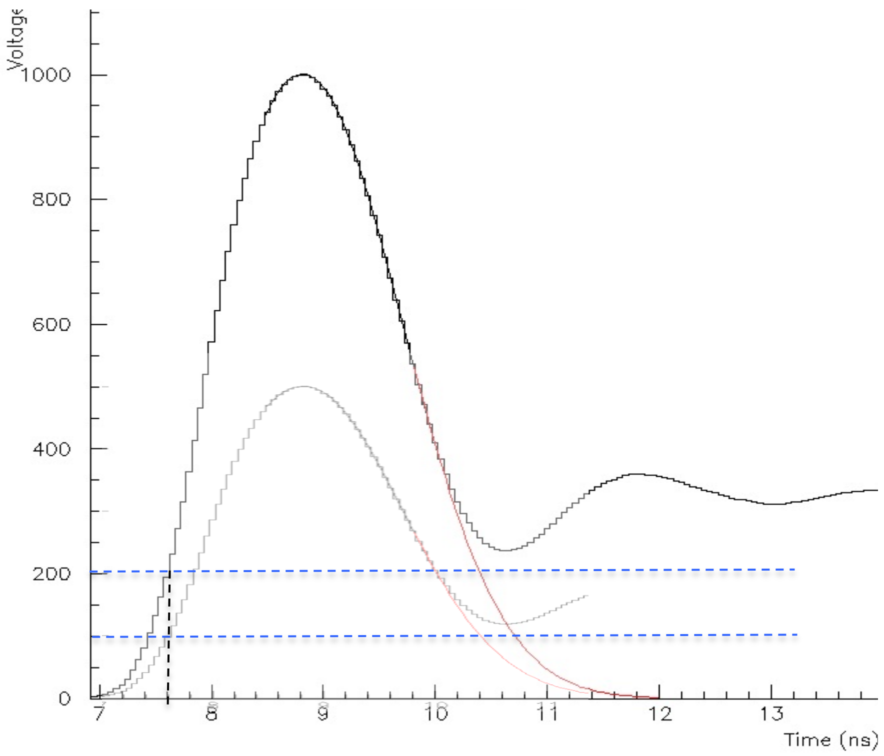

- Define the e-peak arrival time at a Constant Fraction (CFD) of the peak maximum
- CFD Timing minimizes time-walk or “slewing” effects
- CFD Timing of raw pulses suffers from noise
- Is it possible to filter-out the noise?

Signal processing: Fitting the pulse

Fit with the difference of two logistic functions

$$f(t;p_0,p_1,p_2,p_3,p_4,p_5,p_6) = \frac{p_0}{\left(1+e^{-(t-p_1)p_2}\right)^{p_3}} - \frac{p_0}{\left(1+e^{-(t-p_4)p_5}\right)^{p_6}}$$

- ✓ Define the start and the end of the e-peak
- ✓ Define Signal Arrival Time
- ✓ Estimate the charge
- ✓ Neutralize noise effects

Fitting the e-peak waveform helps to estimate the charge in “impossible” cases

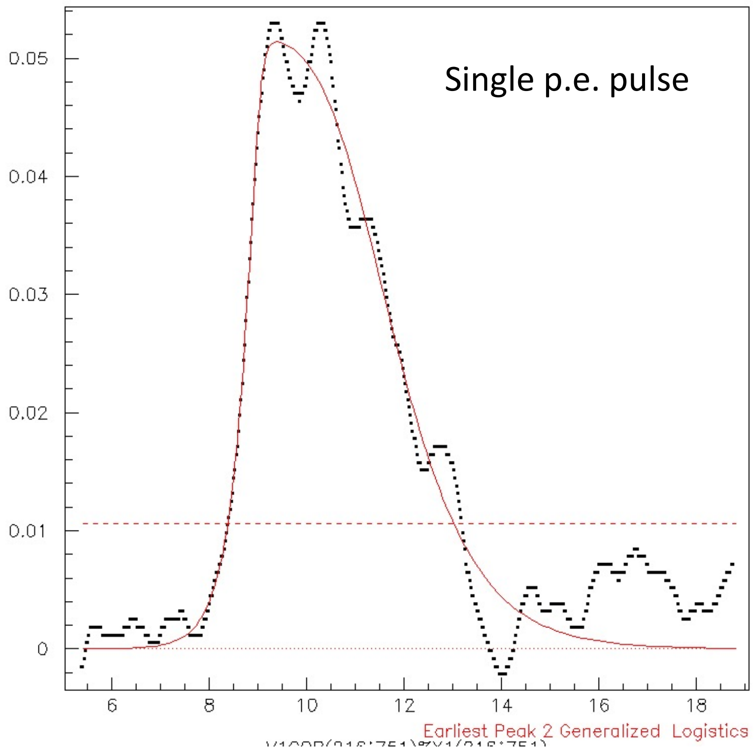

Laser beam: Timing performance

$T_{e\text{-peak}}$ = Signal Arrival Time (SAT)

SAT of a sample of events = <$T_{e\text{-peak}}$ >

Time Resolution = RMS[$T_{e\text{-peak}}$]

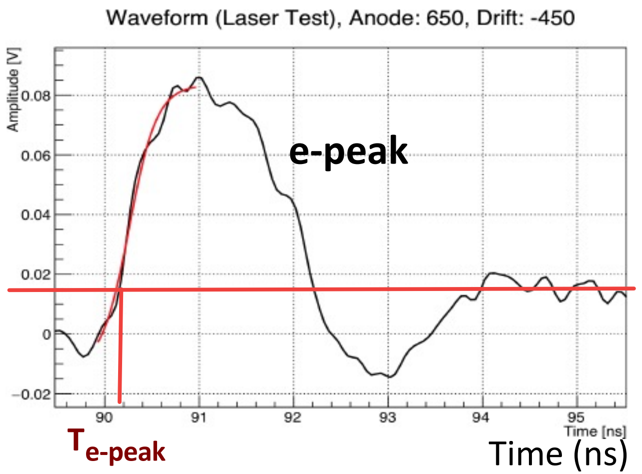

→ Time the signal arrival with **Constant Fraction Discrimination (CFD)** on the fitted noise-subtracted e-peak

CFD @ 20% of the e-peak amplitude

- t_0 reference: fast photodiode (~10 ps resolution)
- Detector response at different field settings
- **Timing resolution 76.0 ± 0.4 ps achieved** @ drift/anode: -425V / +450 V
  - improves strongly with higher drift field, less with anode field

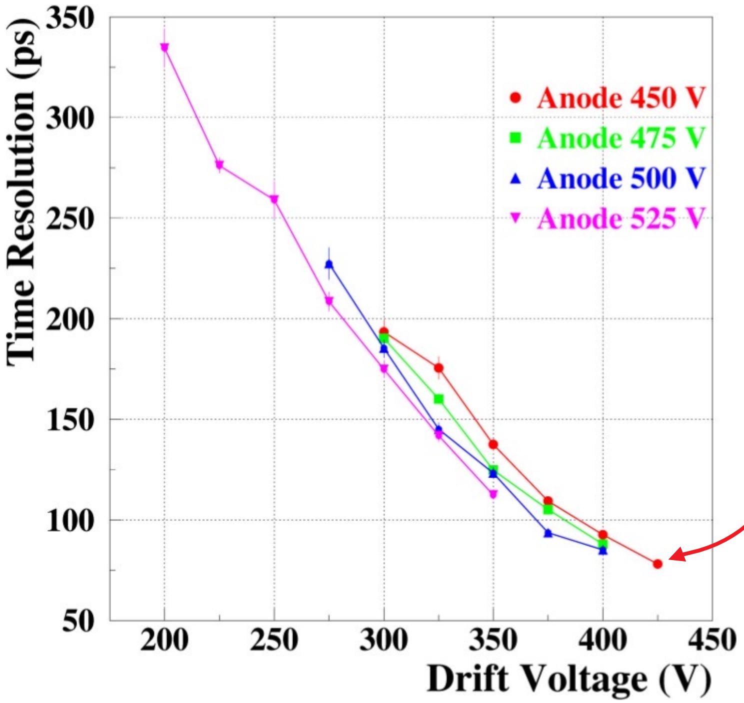

Laser beam: Timing performance

- t_0 reference: fast photodiode (~10 ps resolution)
- Detector response at different field settings
- **Timing resolution 76.0 ± 0.4 ps achieved** @ drift/anode: -425V / +450 V
  - improves strongly with higher drift field, less with anode field

$T_{e\text{-peak}}$ = Signal Arrival Time (SAT)

SAT of a sample of events = <$T_{e\text{-peak}}$ >

Time Resolution = RMS[$T_{e\text{-peak}}$]

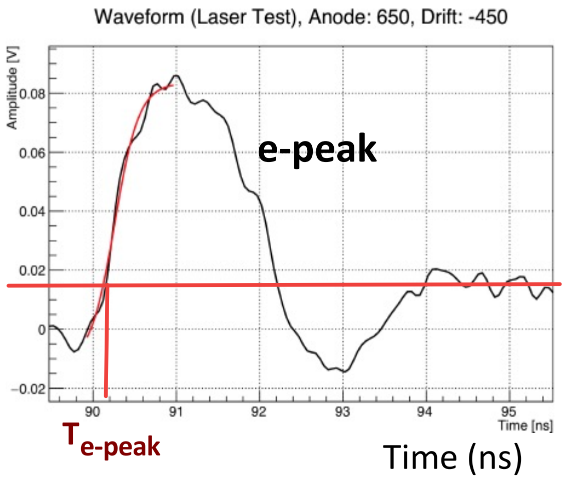

Time Resolution depends mostly on e-peak charge

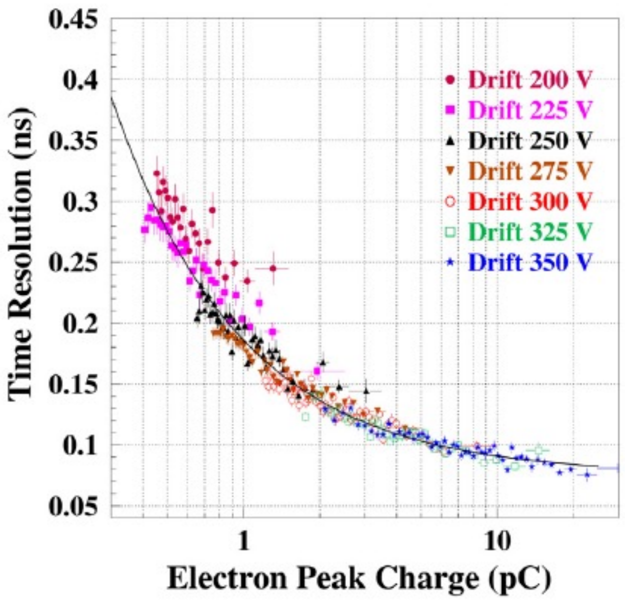

Laser beam: Timing performance

$T_{e\text{-}peak}$ = Signal Arrival Time (SAT)

SAT of a sample of events = $\langle T_{e\text{-}peak} \rangle$

Time Resolution = RMS[$T_{e\text{-}peak}$]

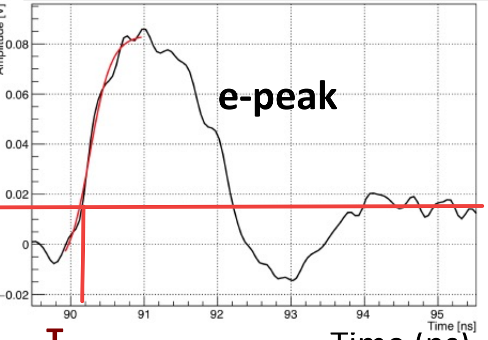

- t_0 reference: fast photodiode (~10 ps resolution)
- Detector response at different field settings
- **Timing resolution 76.0 ± 0.4 ps achieved** @ drift/anode: -425V / +450 V
  - improves strongly with higher drift field, less with anode field

Time Resolution depends mostly on e-peak charge

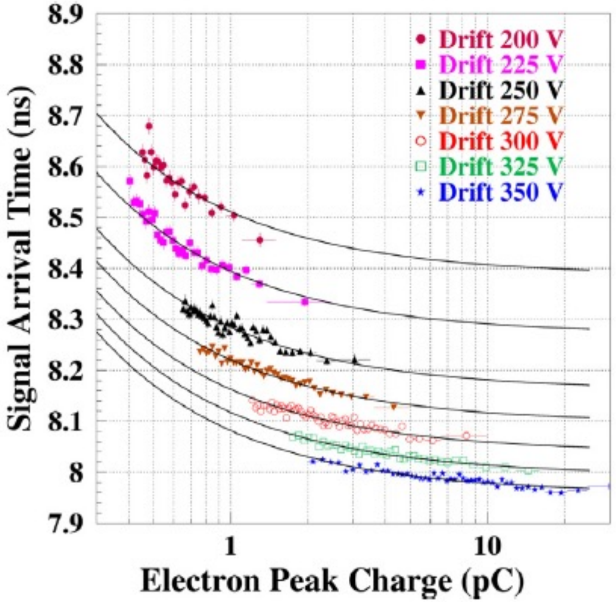

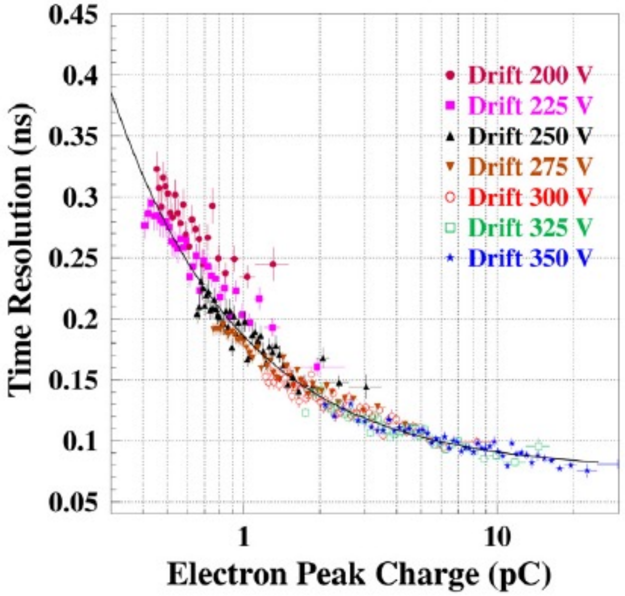

The Signal Arrival Time (SAT) depends non-trivially on the e-peak charge:
- bigger pulses → smaller SAT
- higher drift field → smaller SAT

* Shape of pulse is identical in all cases → timing with CFD method does not introduce dependence on pulse size
* Responsible for this “slewing” of the SAT: **physics of the detector**

1. A precise-timing detector

proof with results of single-channel prototypes
Response to Minimum Ionizing Particles (MIPs)

Testing with Particle Beams @ CERN SPS H4

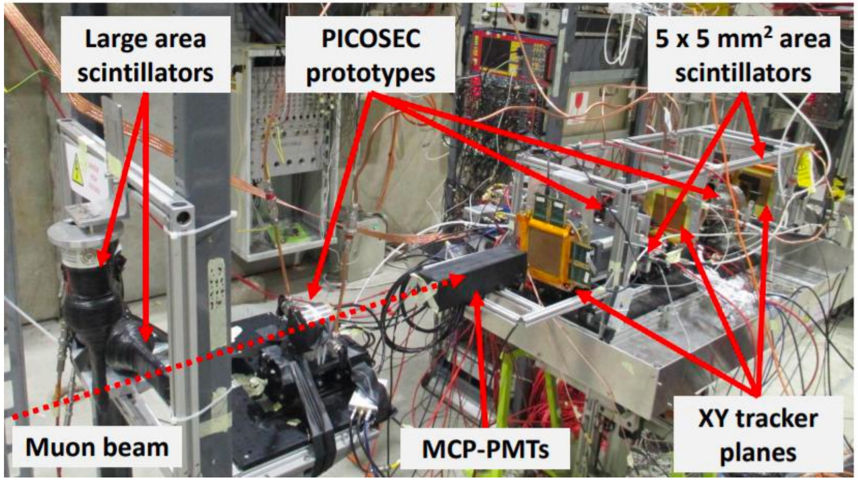

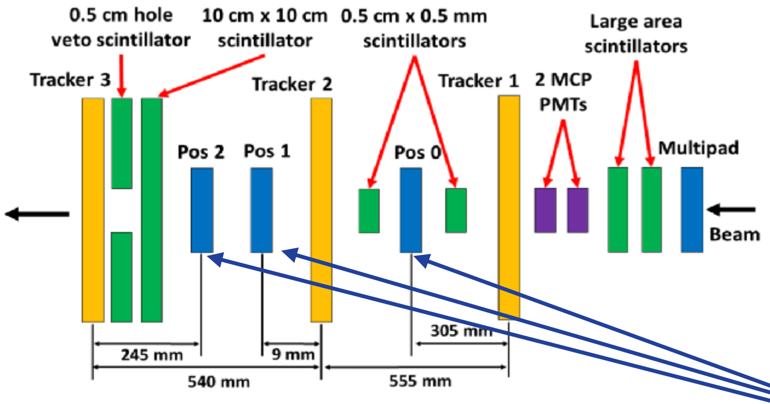

150 GeV muons or pions

- Time reference: two MCP-PMTs (<5 ps resolution).
- Scintillators: used to select tracks & to avoid showers.
- Tracking system: 3 triple-GEMs (40 μm precision).
- Electronics: CIVIDEC preamp. + 2.5 GHz LeCroy scopes.

Several PICOSEC prototypes tested in parallel

Last run Oct. 2018:
Next run late 2021(?)

Time resolution for MIPs

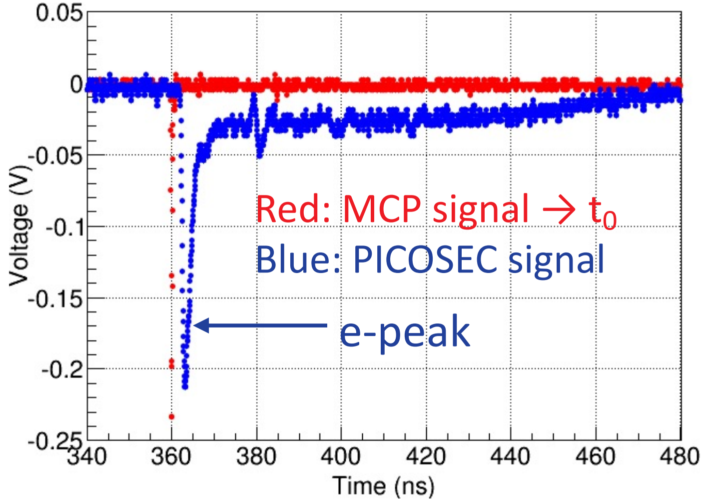

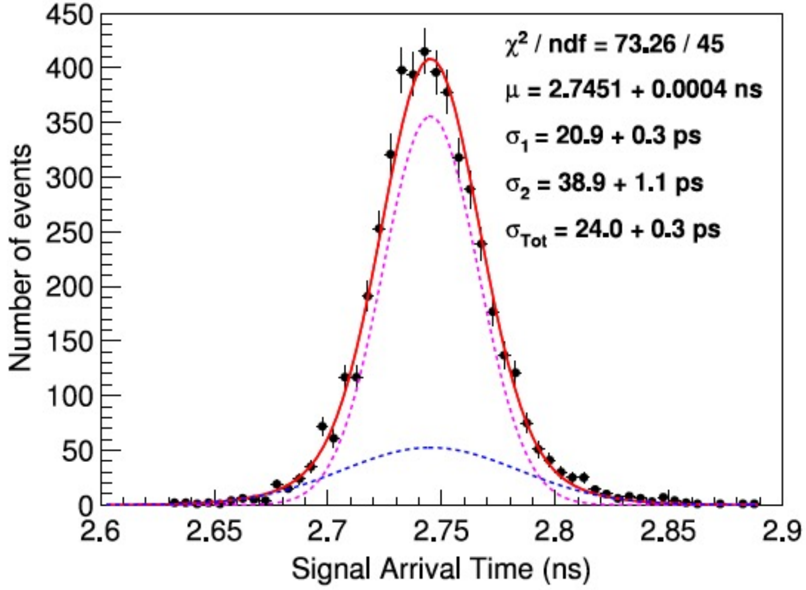

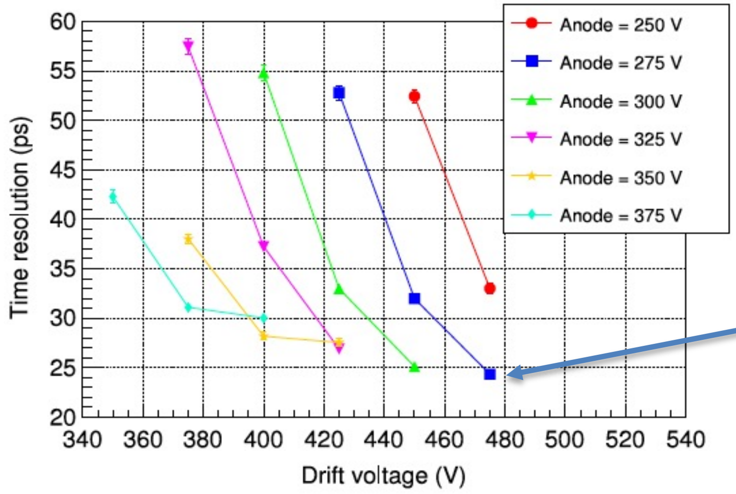

- Same detector as for Laser tests (MgF_2 radiator, CsI photocathode, Bulk MicroMegas, COMPASS gas)
- **Best time resolution: 24.0±0.3 ps**
- **@ Drift/Anode: -475V/+275V**

J. Bortfeldt et. al. (RD51-PICOSEC collaboration), Nuclear. Inst. & Methods A 903 (2018) 317-325

2. A well understood detector

detailed simulations and modeling

Detailed simulation

Use **Garfield++** to simulate PICOSEC for single photoelectrons, **ANSYS** for the electric field

Anode voltage does not affect much the timing properties of the signal. So, we split the simulation in three stages:

Anode: 450 V , E = 35 kV/cm

Cathode: 300-425 V , E =[15, 21] kV/cm

1) Drift region: simulation till the mesh.

2)Simulation in the amplification region

3) Electronics

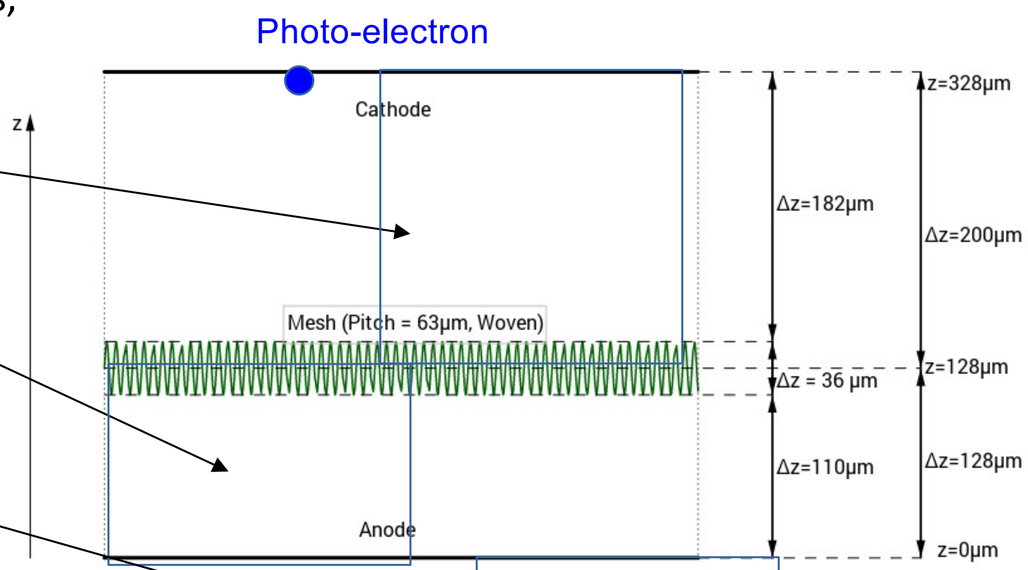

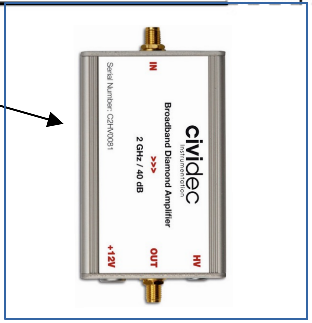

Each photoelectron produces **10^{5} – 10^{6}** other electrons: A simulation of the amplification region as well would be very time-consuming (~months, to cover the various voltage etc settings tried).

http://ikee.lib.auth.gr/record/297707

Detailed simulation: Stage 1 – Drift region

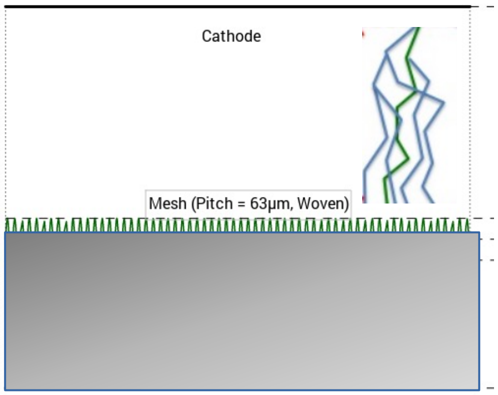

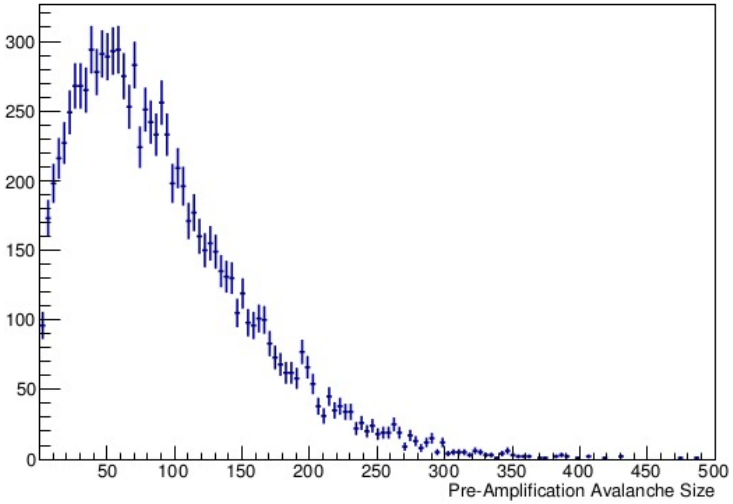

We start with one photoelectron,
and we follow the avalanche it creates
till the mesh.

We then count:
- **how many** electrons pass the mesh and **when**

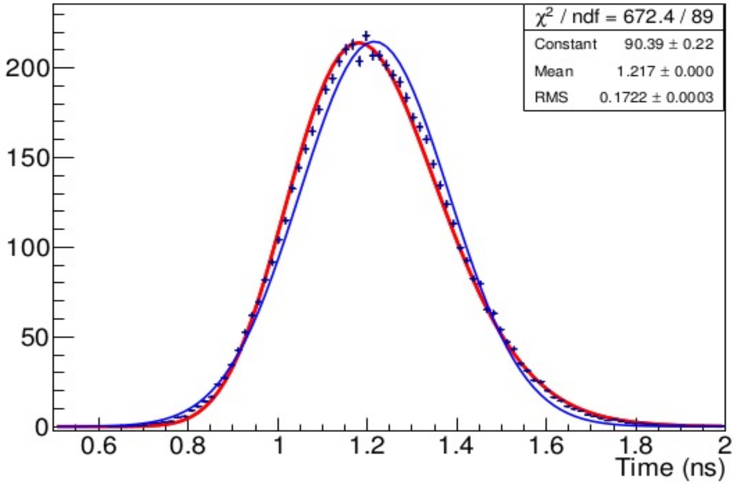

Detailed simulation: Stage 2 – Amplification Region

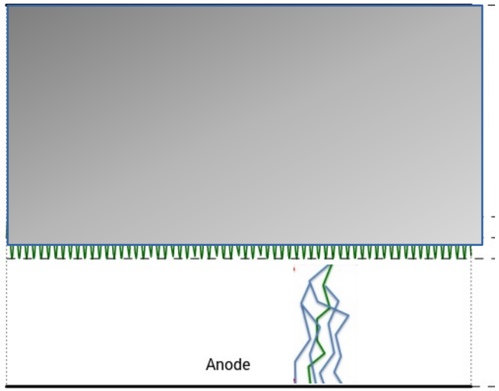

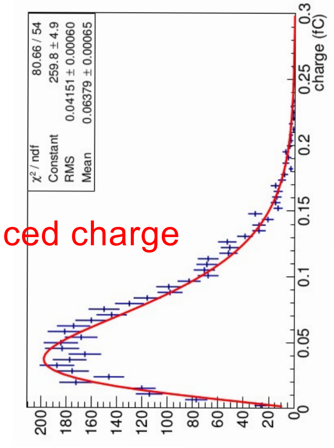

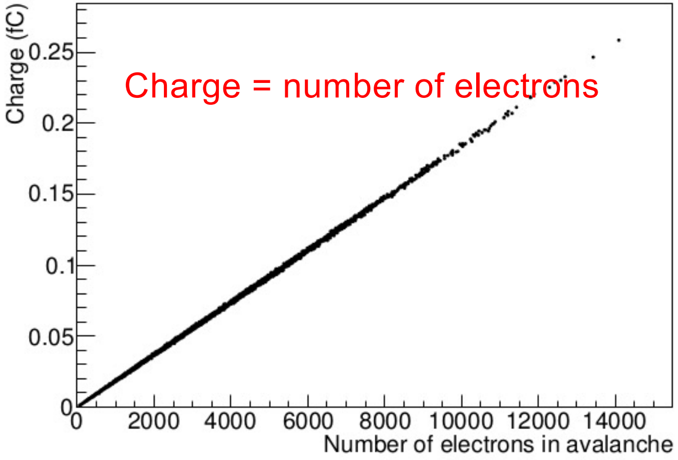

For each electron passed through the mesh:

- Follow the avalanche it produces in the amplification region
- Count **how many electrons** arrive on the anode and the **induced charge**: <u>**one-to-one correspondence**</u>

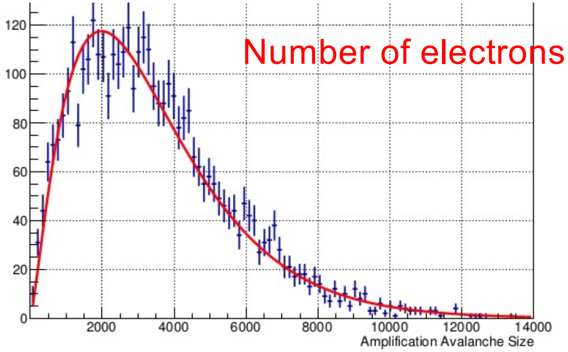

The distribution fit nicely with a Polya (red)
→ for each electron passing the mesh, we get a representative number of electrons on the anode, by picking randomly from this Polya.

Detailed simulation: Stage 3 – Response of electronics

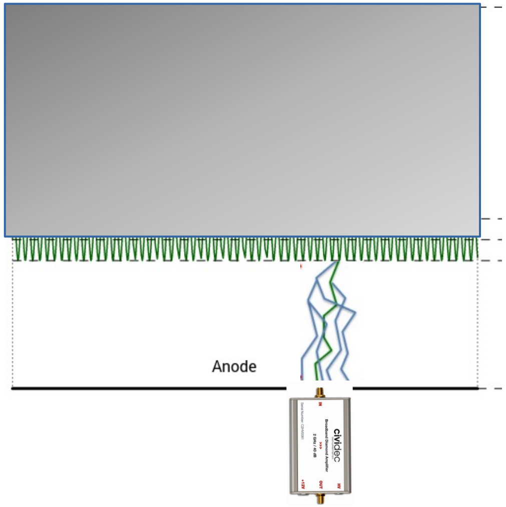

- Assume simulated pulse is described with the difference of two logistics
- Find the parameters by using experimental data, in a statistically coherent way:
  a) Describe the pulse shape produced from one electron passing the mesh and entering the amplification region. Take distributions of "mean arrival times" for the electrons reaching the anode (from Garfield++) and convolute them with the shape of the electronic response, and
  b) Compare the result with the average waveform observed in the experimental data.

$$\frac{\langle S(t)\rangle_{Q_{tot}=Q}}{Q} = \int_0^{\infty} f(t-\tau)\,\langle \Phi(\tau)\rangle_{Q_{tot}=Q}\, d\tau$$

Normalized waveform

Average waveform / its total charge (experimental data) = Response function of the electronics with all gains=1 (convolution) * Distribution of Mean Arrival times (simulation)

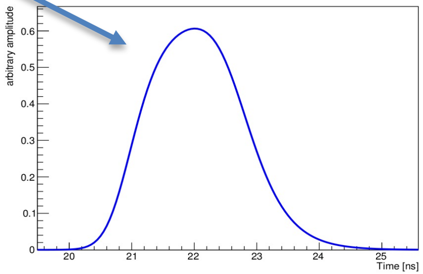

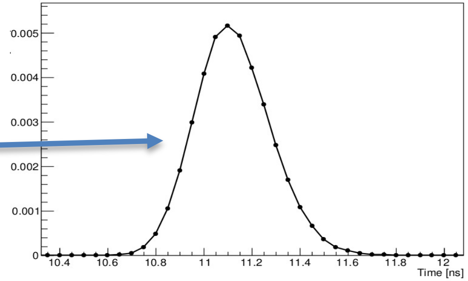

Detailed simulation: Electronic gain

Pulse generation in Garfield++ –no extra electronic gain

N electrons pass through the mesh at times **τ_1, τ_2, …, τ_N**

$$S(t) = \sum_{i=1}^{N} q_i \cdot f(t - \tau_i)$$

Each one of these N electrons contributes a pulse **f(t)** (previous slide), **displaced by the respective time τ_1, τ_2, …, τ_N,** where the size of the pulse is put as a random variable drawn from the Polya describing the avalanche population (or the induced charge, equivalently).

We thus, produce pulses with shapes like those in the experiment, but:

$f(t-\tau_i)$ is the shape of the electronics response: in order the simulated pulses to be exactly like in the data, we need the Gain, G, of the electronics in order to construct **G*S(t)**

Pulse generation in Garfield++ – including electronic gain

G should be a constant. But…

Experiment
Simulation

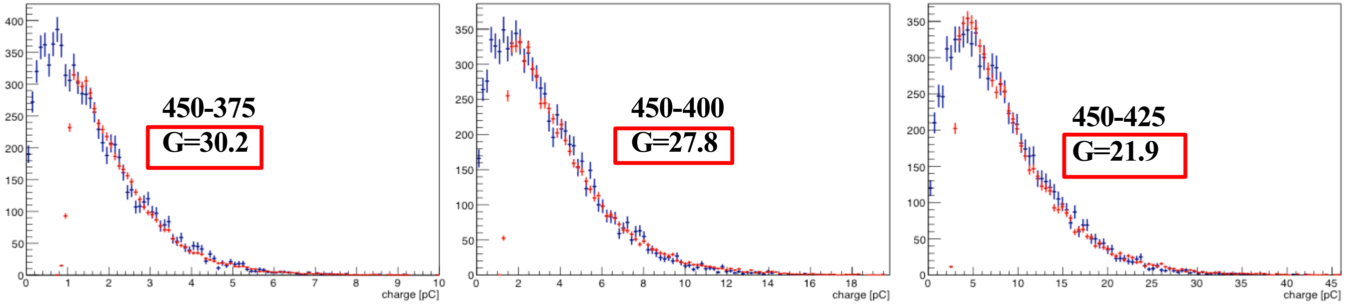

Detailed simulation: Electronic Gain

→ There must be another phenomenon not included here...
In Garfield++ , all interactions between electrons and molecules are included, but not between molecules themselves.
But Ne has excited states at high enough energies, that, when de-exciting, can cause the ionization of C_2H_6.

$$Ne^* + C_2H_6 \rightarrow Ne + C_2H_6^+ + e^-$$

Such indirect ionizations are called the **"Penning effect"**

By putting as a free parameter, the probability, **r**, to have such an excited Ne to cause an ionization, we found that the value of **r=50%** for the **"Penning Transfer Rate"** allows to use a constant electronic gain G, independent of the voltage in the drift region.

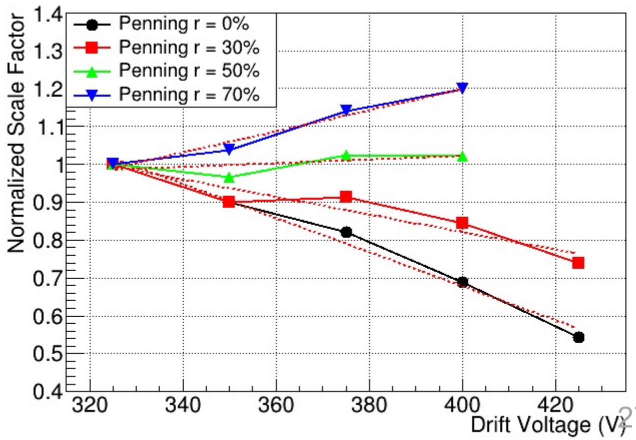

Detailed simulation with “trimmed” Garfield++

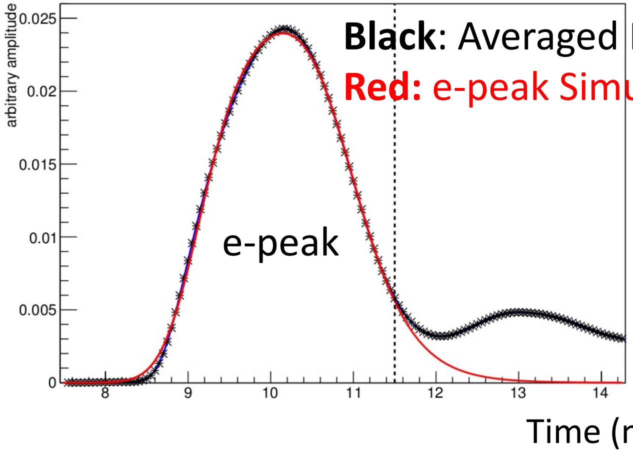

Black: Averaged PICOSEC waveforms in a certain e-peak charge region

Red: e-peak Simulation Prediction (Garfield++ and Electronics Response)

All behaviors seen in single p.e. laser data are also seen in these detailed Garfield++ simulations!!!

The Signal Arrival Time (SAT) depends non-trivially on the e-peak size:

* bigger pulses
  → smaller SAT
* higher drift field
  → smaller SAT

* Time resolution depends mostly on e-peak charge

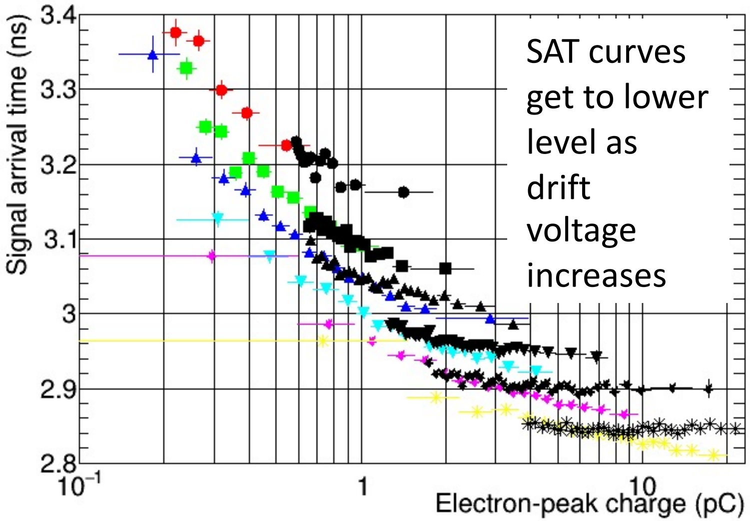

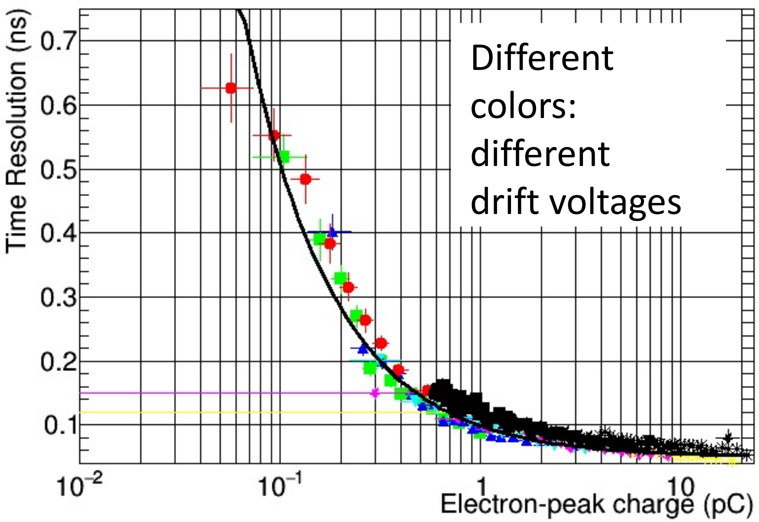

Color: Simulation – Black: Data

Detailed simulations: under the hood

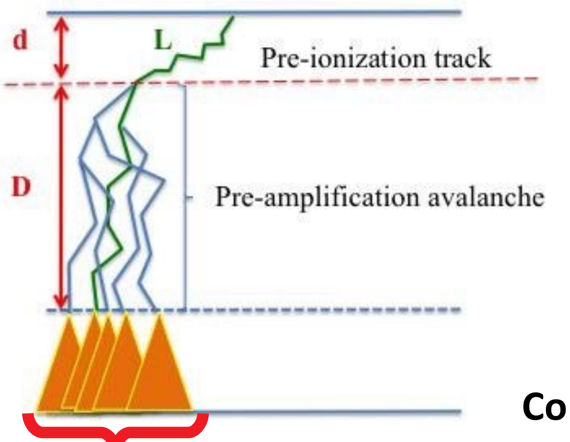

Gives e-peak pulse

Microscopic equivalent to e-peak's SAT = Mean Time (T) of all electron arrival times on the mesh

*** <SAT> linear with <T>**

*** RMS(SAT) linear with RMS(T)**

Correspondence of experimental Observables to Relevant Microscopic Variables

Sets of avalanches of a certain e-peak charge

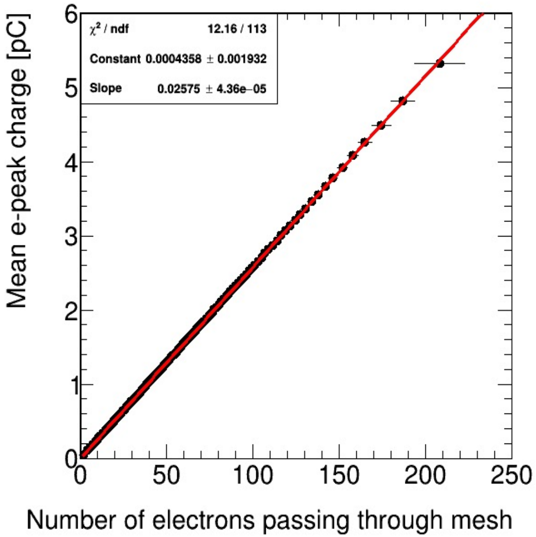

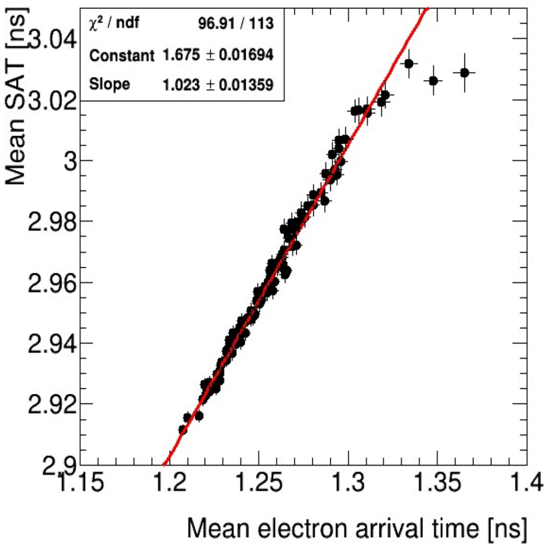

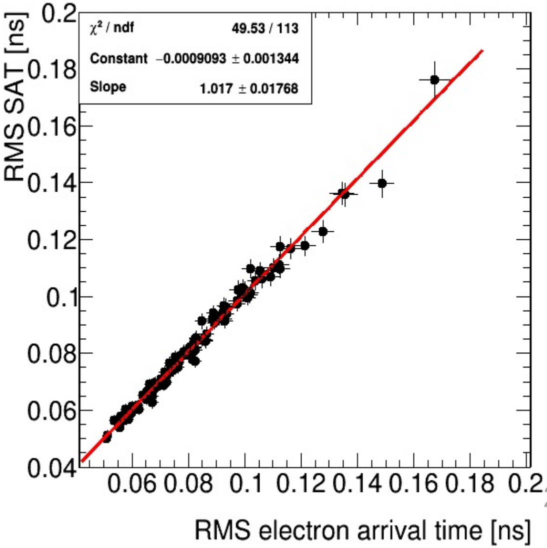

Detailed simulations: under the hood

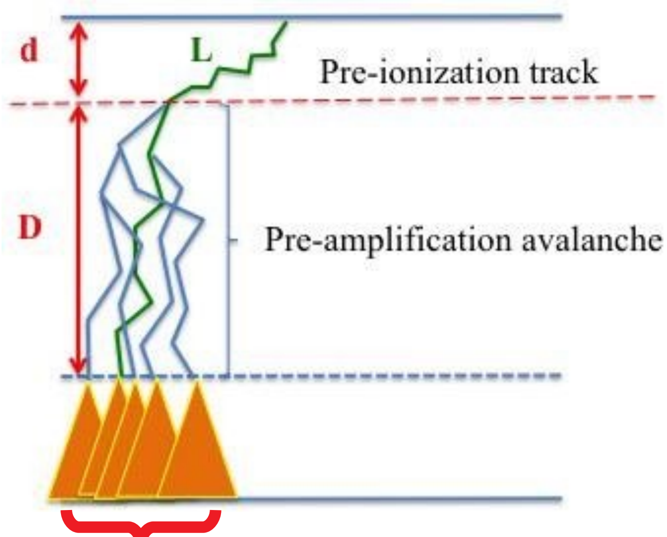

Total arrival time reduces with avalanche length

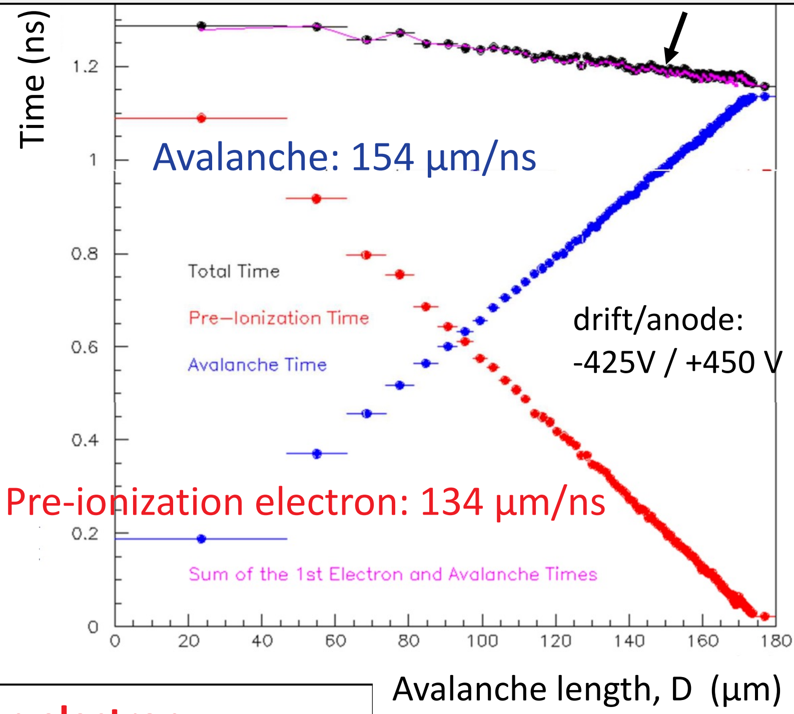

Avalanche runs with higher drift velocity than **pre-ionization electron**
So, SAT "slewing" seen in single p.e data is explained:
SAT reduces with avalanche length
Long avalanches → big e-peak charge
} **SAT reduces with e-peak charge** !

Let us be inspired by the phenomenon of "Quenching"

From Rob Veenhof

Electrons in Ar/CO_2 at E=1 kV/cm

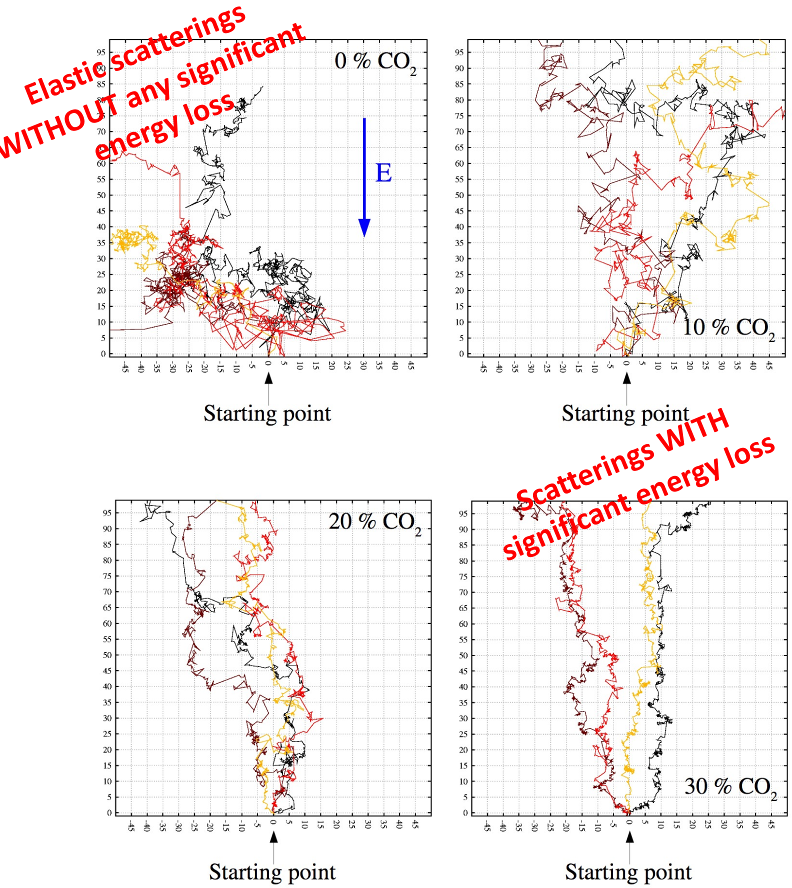

In the case of "quenching", the energy loss results in higher drift velocity !!!

Let us be inspired by the phenomenon of "Quenching"

From Rob Veenhof

Electrons in Ar/CO_2 at E=1 kV/cm

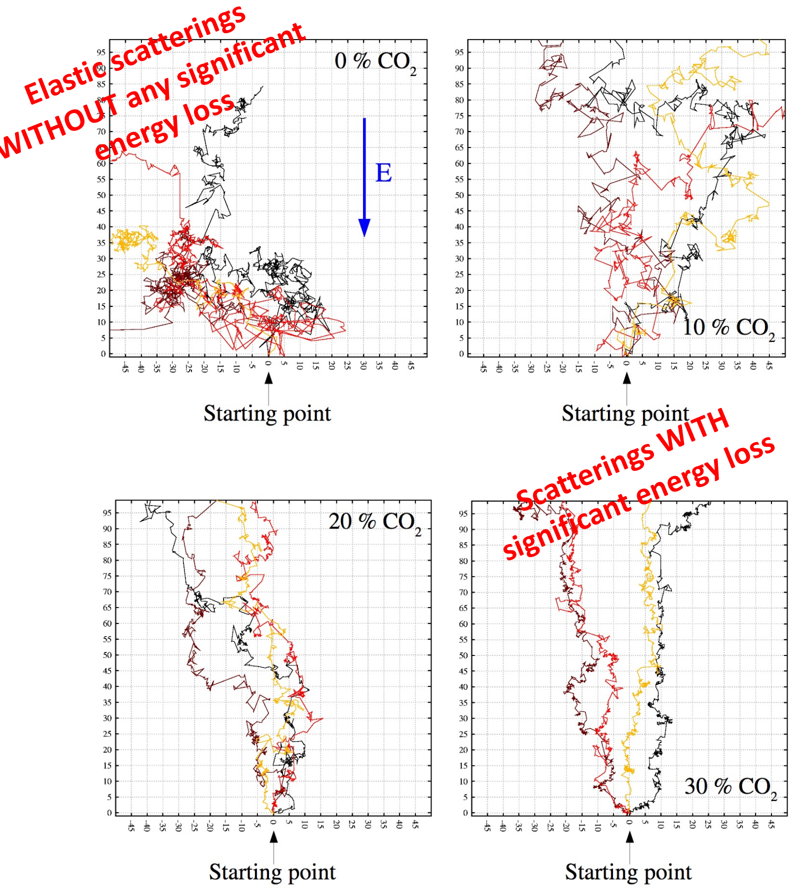

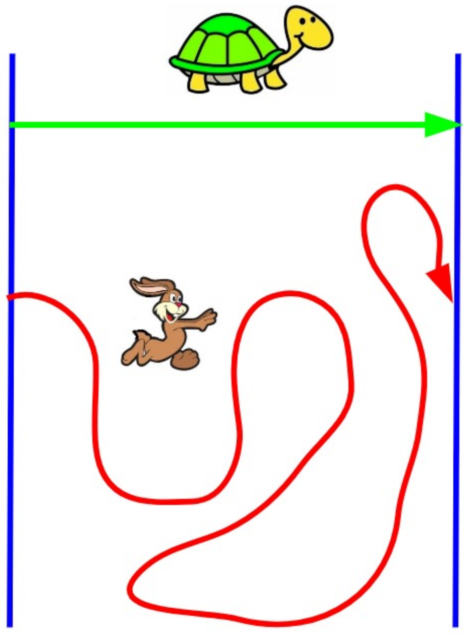

In the case of "quenching", the energy loss results in higher drift velocity !!!

Phenomenological model: A deeper looking under the hood

- An ionizing electron in the avalanche, every time it ionizes, will gain a time **ξ** relative to an electron that undergoes elastic scatterings only.
- A new produced electron by ionization starts with low energy, suffers less delay due to elastic backscattering compared to its parent. Relative to his parent it will have a time-gain **ρ**
- Parameters **ξ** and **ρ** should follow a joint probability distribution determined by the physical process of ionization and the respective properties of interacting molecules

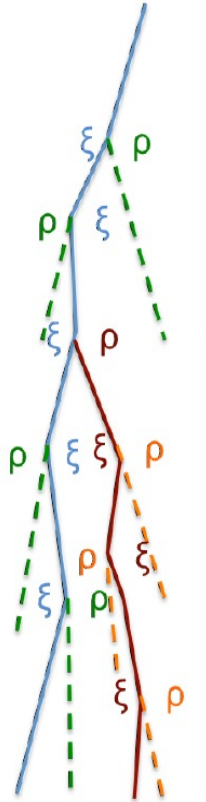

J. Bortfeldt et al. for the PICOSEC Collaboration, NIM-A, Vol. 993, (2021), 165049 - arXiv:1901.10779

Understood in terms of phenomenological model

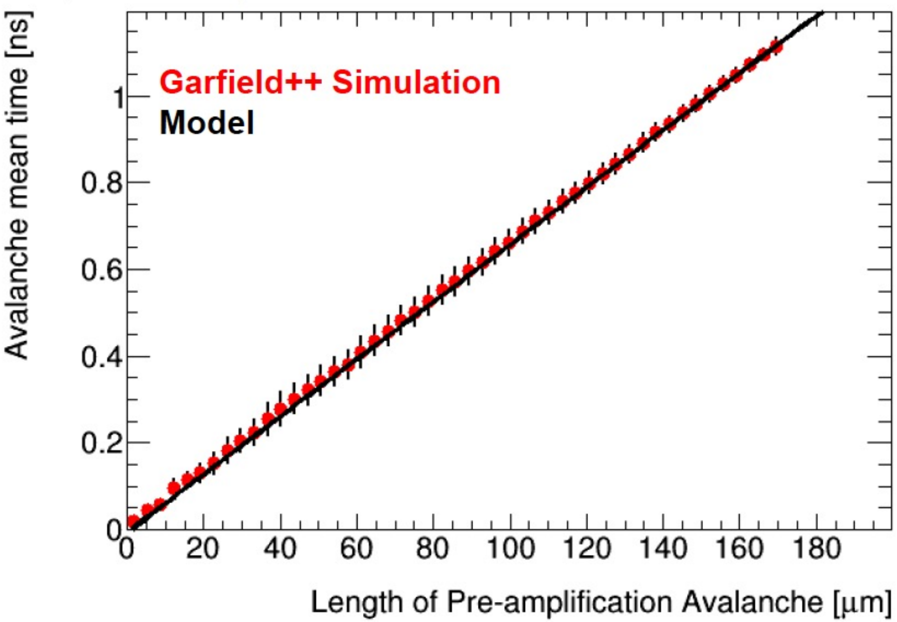

We can predict the effective drift velocity of the avalanche

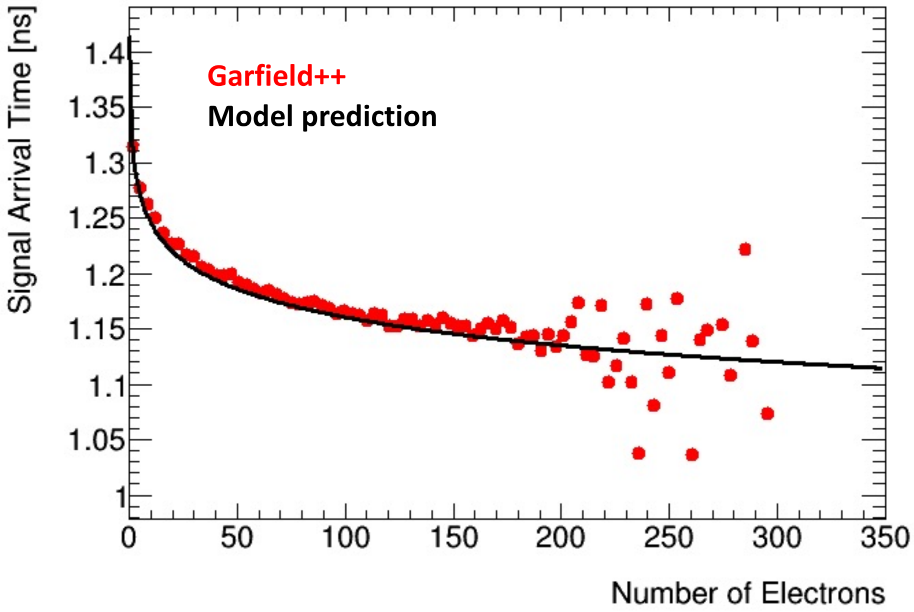

We can describe and explain the SAT dependence on the number of avalanche's electrons (i.e. on the e-peak size)

- The other parameters of the model are: the drift velocity of the photoelectron and the first Townsend coefficient.
- The model treats the number of electrons in an avalanche as continue variable.

Understood in terms of phenomenological model (2)

We can describe and explain the Resolution dependence on the length of the avalanche and on the number of avalanche's electrons (i.e. on the e-peak size)

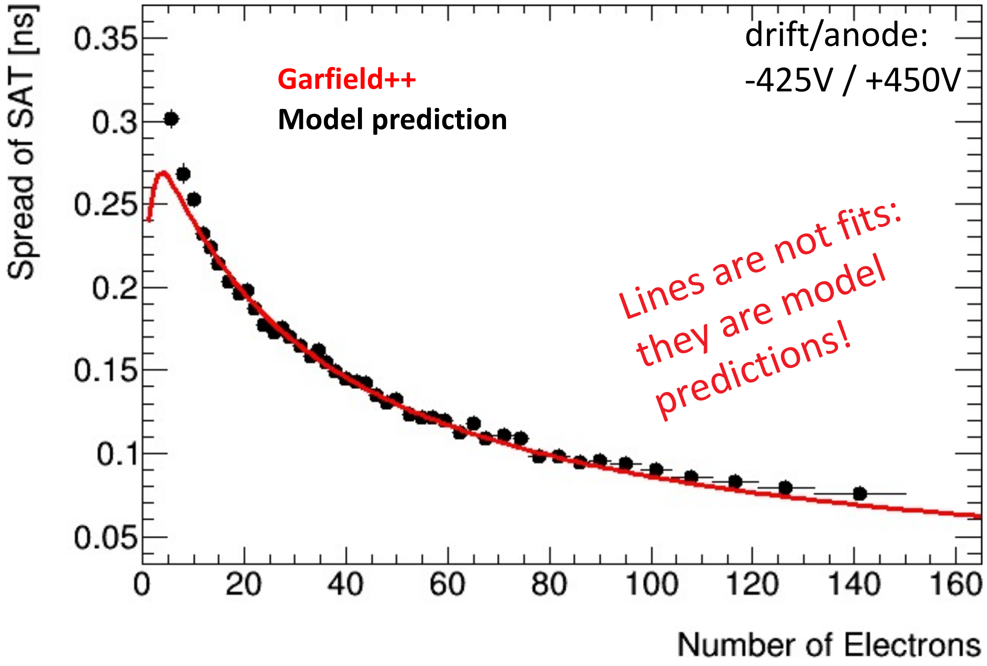

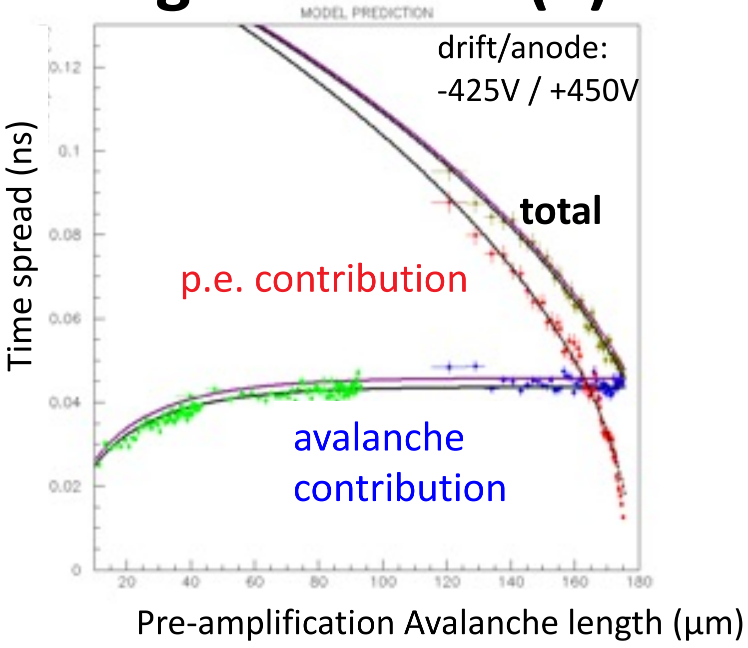

The model describes SAT and Resolution
a) vs. avalanche length &
b) vs. number of electrons in avalanche
(i.e, vs. e-peak charge)

→ Before and after the mesh

Not only averages and RMS, but full distributions, vs. values of operational parameters (e.g., drift voltage)

3. Estimation of the No of p.e. per MIP

A consistent and unbiased procedure to estimate the photocathode yield per MIP (1)

Precise alignment based on the charge-weighted beam profile

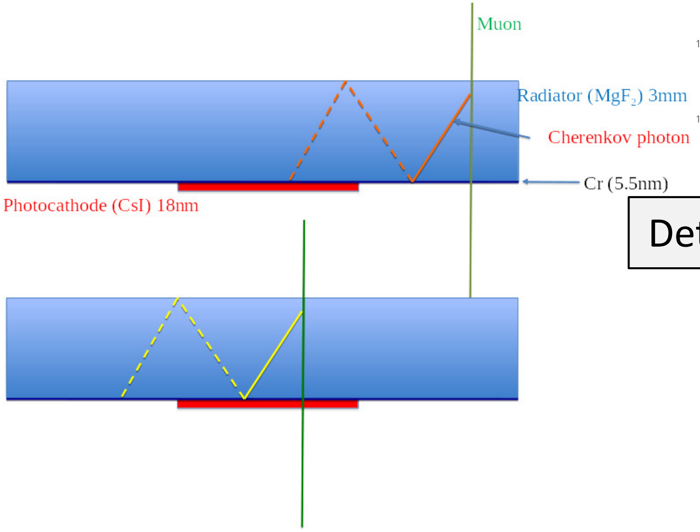

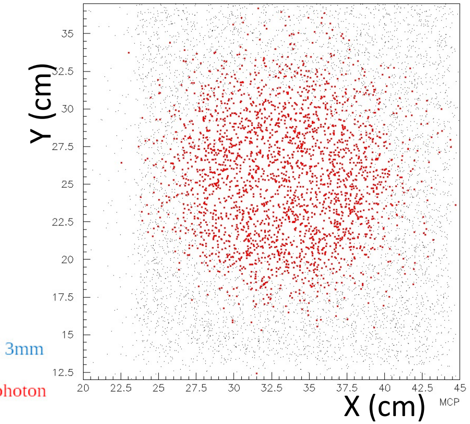

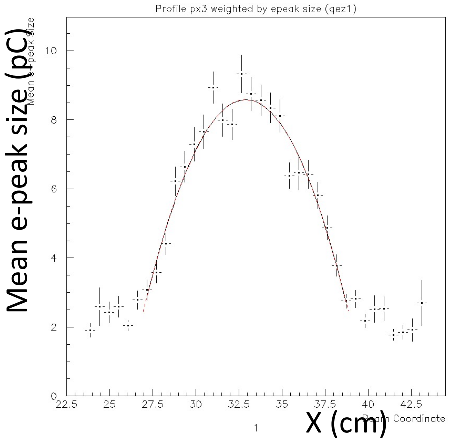

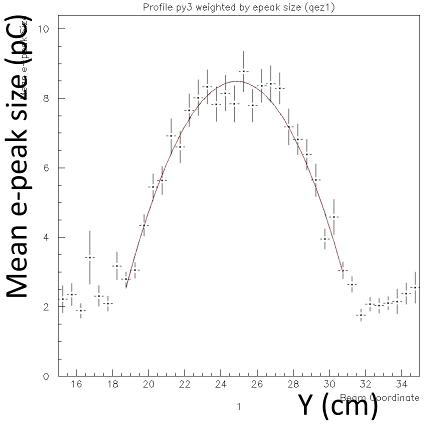

Determination of the anode geometrical acceptance taking into account reflections

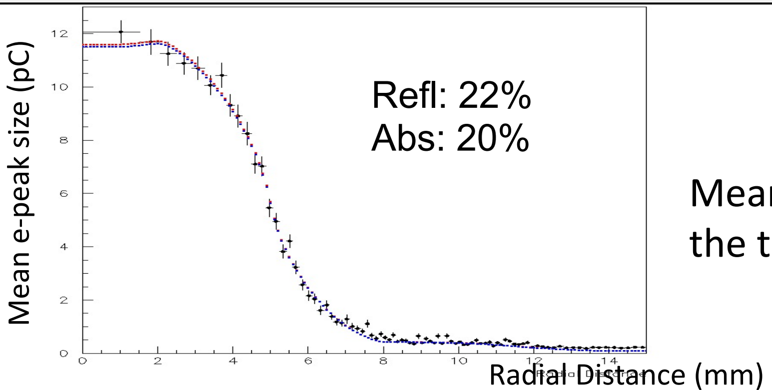

Mean charge per track (pC) vs the track radial distance (mm)

A consistent and unbiased procedure to estimate the photocathode yield per MIP (2)

Determination of the charge distribution parameters when the **PICOSEC MM responds to a single-pe** using UV calibration data

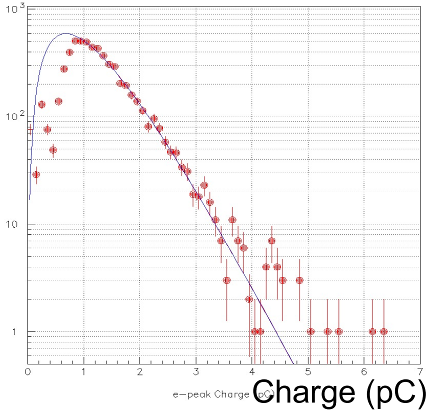

A Polya fit to the single-p.e. charge distribution

$$P_{spe}\left(Q; a=b=\theta+1, \bar{Q}_e\right)dQ = \frac{1}{Q_e}\frac{(\theta+1)^{(\theta+1)}\left(Q/\bar{Q}_e\right)^{\theta}}{\Gamma(\theta+1)}e^{-(\theta+1)Q/\bar{Q}_e}dQ$$

$$E\left[Q_{spe}\right] = \bar{Q}_e = \langle Q_e \rangle$$

$$V\left[Q_{spe}\right] = \frac{1}{\theta+1}\langle Q_e \rangle^2 = RMS^2$$

Fit the charge distribution of the PICOSEC **response to muons**

If N is the mean number of pes produced per muon track, then a muon passing through the radiator at distance R from the anode center will result to a PICOSEC signal with charge Q.

Q follows a p.d.f. F(Q,R;N) which can be expressed using the geometrical acceptance A(R), as a convolution of a Poissonian distribution with mean N·A(R)

$$\Pi(N_{pe}; N, A(R)) = \frac{[N \cdot A(R)]^{N_{pe}}}{N_{pe}!} \cdot \exp[-N \cdot A(R)]$$

and the multi-Polya distribution

$$P(Q; N_{pe}, \theta, \overline{Q_e}) = \underbrace{P_{spe} \otimes P_{spe} \cdots \otimes P_{spe}}_{N_{pe}\ times} = \frac{1}{\overline{Q_e}} \frac{(\theta+1)^{N_{pe}(\theta+1)} (Q/\overline{Q_e})^{N_{pe}(\theta+1)-1}}{\Gamma(N_{pe}(\theta+1))} \cdot \exp[-(\theta+1) \cdot Q/\overline{Q_e}]$$

as

$$F(Q, R; N) = \sum_{N_{pe}=0}^{\infty} \Pi(N_{pe}; N, A(R)) \cdot P(Q; N_{pe}, \theta, \overline{Q_e})$$

A consistent and unbiased procedure to estimate the photocathode yield per MIP (3)

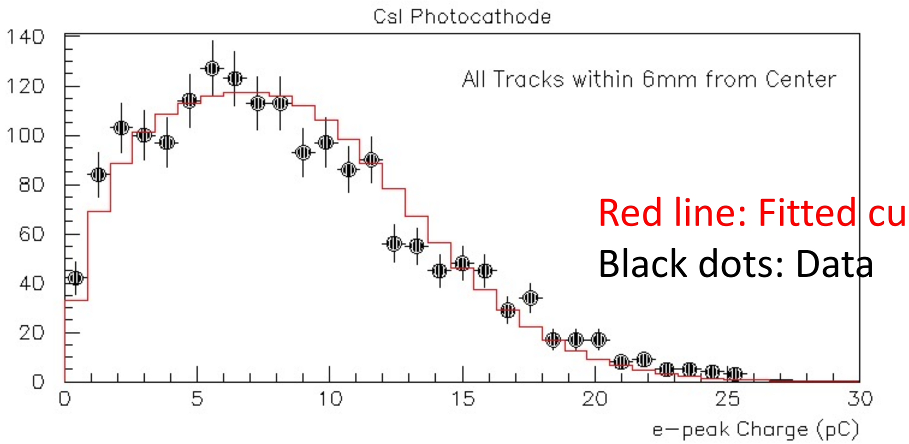

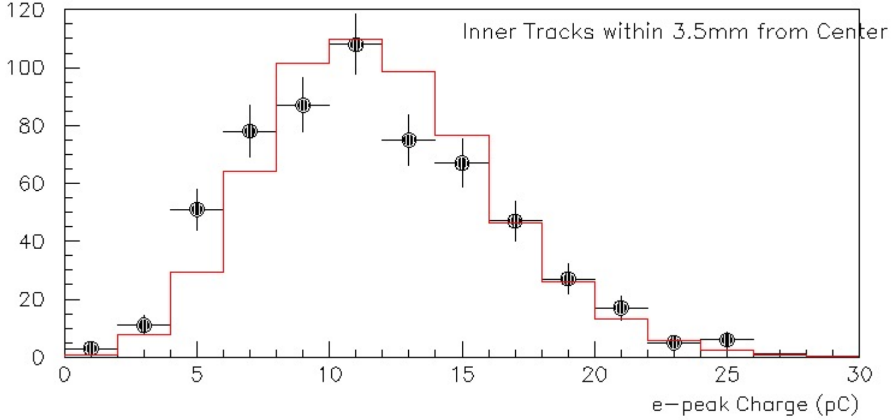

11.5 ±0.4(stat)±0.5(syst) photoelectrons per muon track

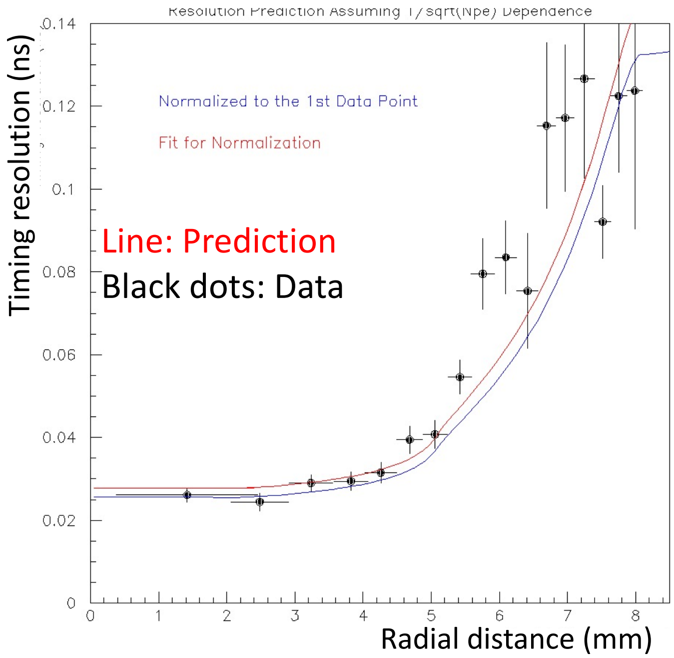

Resolution prediction vs distance from the anode center, assuming **1/sqrt(Npe)** dependence

I Manthos et al 2020 J. Phys.: Conf. Ser.1498 012014

4. Scaling the PICOSEC concept for HEP applications

Detector stability

Photocathode robustness

Large area coverage

Detector stability – Resistive Micromegas

Best resolution was at voltages which give high currents on anode: **robust anode**

Time resolution

Resistive strips

σ = 41 ps

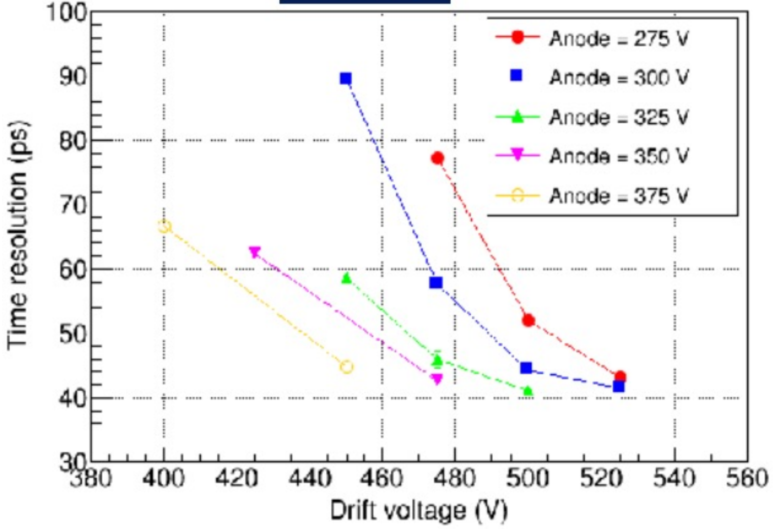

Floating strips

σ = 28 ps

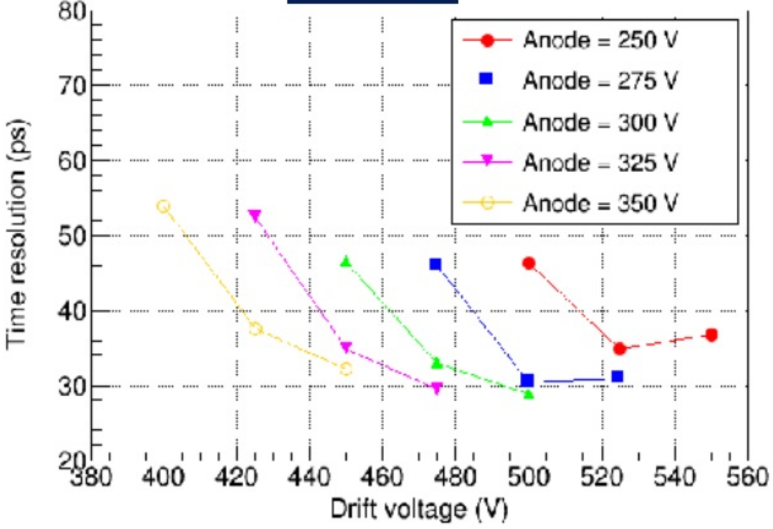

Beam results with protected anodes

- Results not far from the PICOSEC bulk readout
  - Resistive strips: **41 ps** (10MΩ/□), **35 ps** (300 kΩ/ □)
  - Floating strips: **28 ps** (25 MΩ)

Photocathode robustness – Problems with CsI

Photocathode robustness preserves QE and thus detector efficiency and timing resolution during long-period operation

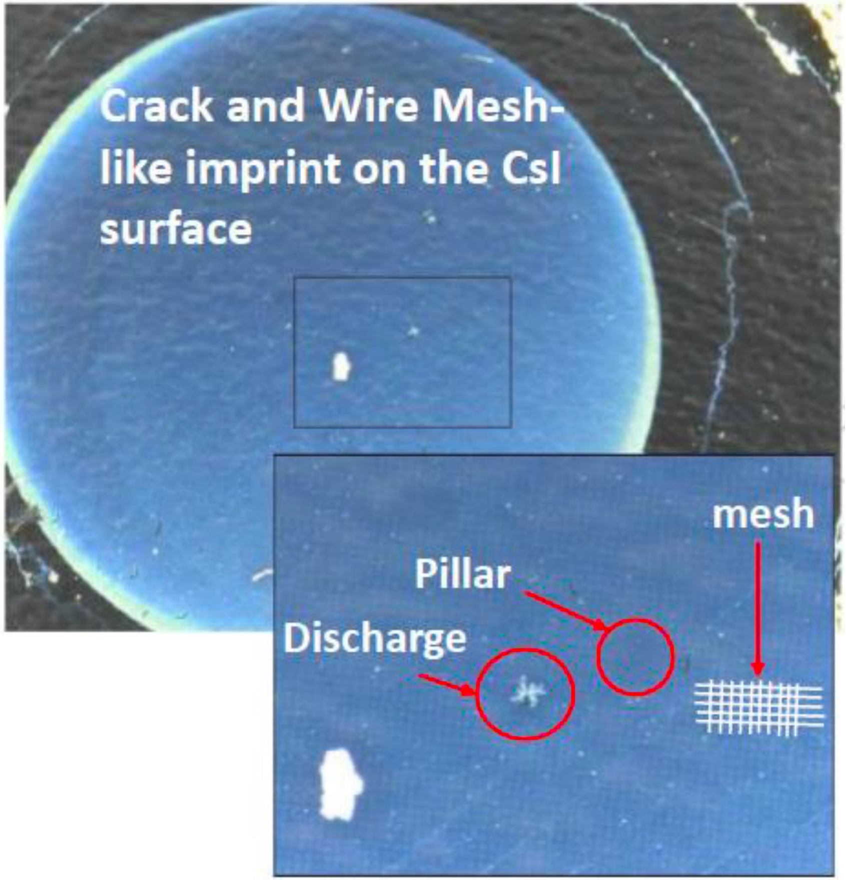

CsI sensitive to humidity, ion backflow and sparks

- **Protection layers on CsI** and **alternative photocathode materials** (Metallic, DLC, B_4C,nano diamond powder, CVD diamond) were tested
- For each material, the working point with the best time resolution has to be determined
- Inherently robust materials, but with lower QE

Photocathode robustness – Alternative materials

3mm MgF_2 + DLC of different thicknesses

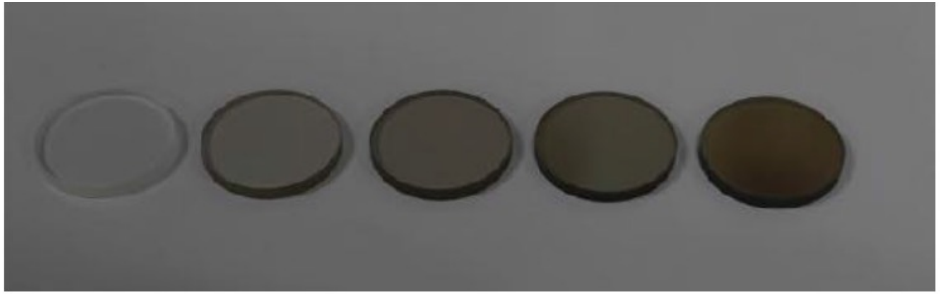

Most promising performance results for non-CsI are from **Diamond-Like Carbon (DLC)**, which also seems robust:

- atmospheric conditions for a few months
- irradiated with pions, in a resistive MM prototype →minimal reduction of Npe/MIP

Thickness of DLC film (nm)	Npe/per muon	Detection efficiency for muons
1	Bad	Bad
2.5	3.7	97%
5	3.4	94%
7.5	2.2	70%
10	1.7	68%
5 nm Cr + 18 nm CsI	7.4	100%

Xu Wang et al, MPGD 2019

2.5 nm DLC in Bulk MM

A/D Voltage	Time Res. (ps)
250/550	37
250/575	34
275/525	38
275/550	34
300/500	39
300/525	34

PRELIMINARY

Application driven R&D investigates more materials (GaN, pure metallic photocathodes)

Large-area coverage - Multi-pad PICOSEC

- Like the single-pad (MgF_2/CsI/bulkMM/COMPASS gas) PICOSEC which achieved 24ps per MIP
- Hexagonal pads 5mm side
- Readout 4 pads → 2 oscilloscopes

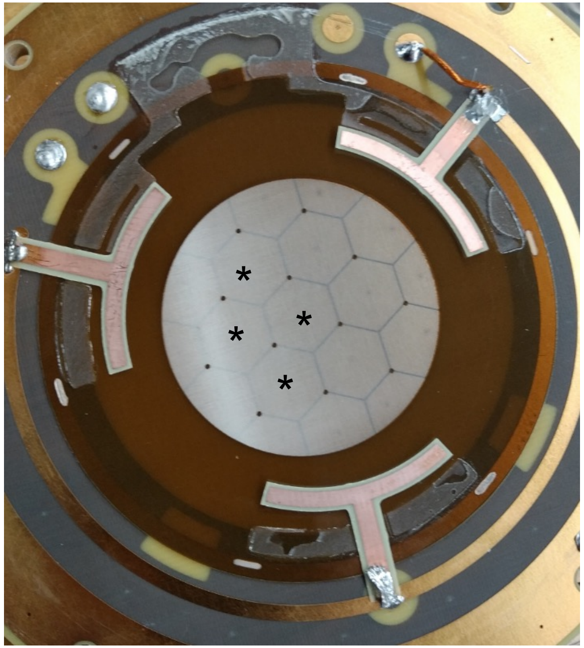

The exact position of each participating pad is needed in order to calculate the combined time resolution

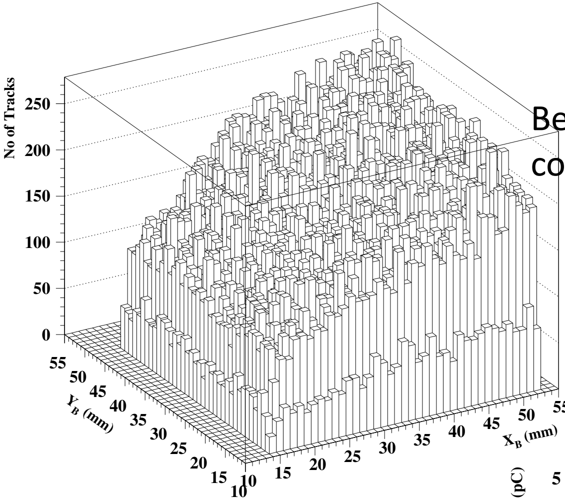

Beam profile that illuminated the area covering all PICOSEC instrumented pads

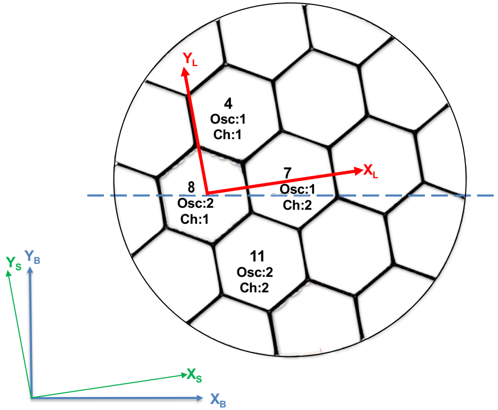

Mean value of the electron peak charge for pad #7

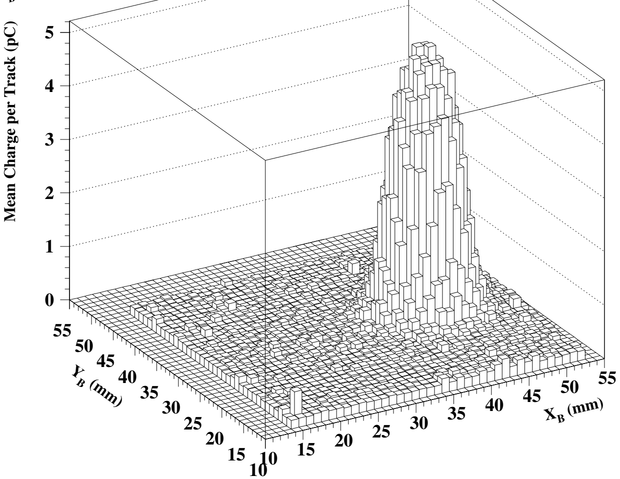

Multi-pad MicroMegas- Individual pad response

- Study response vs. R : distance of track impact from pad center
  - 0<R<2mm: full Cherenkov cone (3mm) inside pad
  - 2 < R < 4.33mm: Cherenkov cone (3mm) mostly inside pad
  - 4.33 < R < 7.5mm: Cherenkov cone (3mm) mostly outside pad

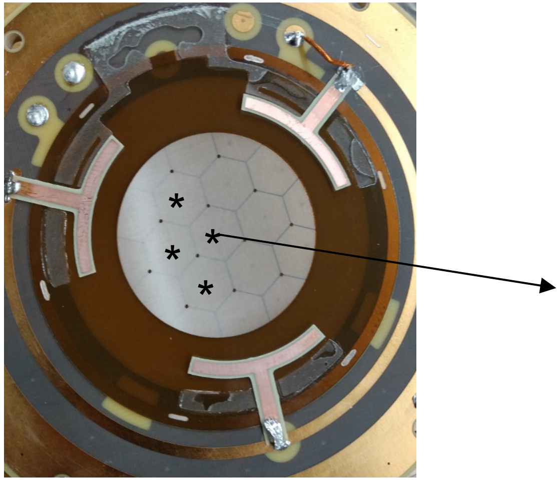

Hexagonal pads 5mm side

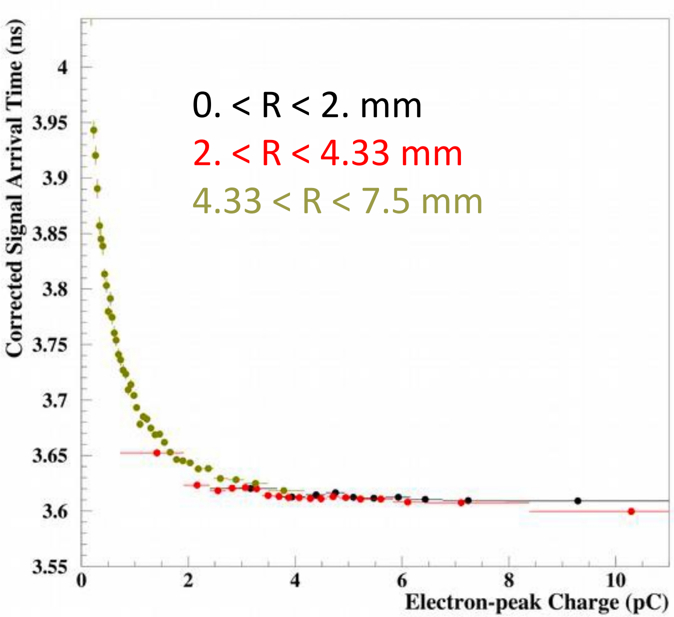

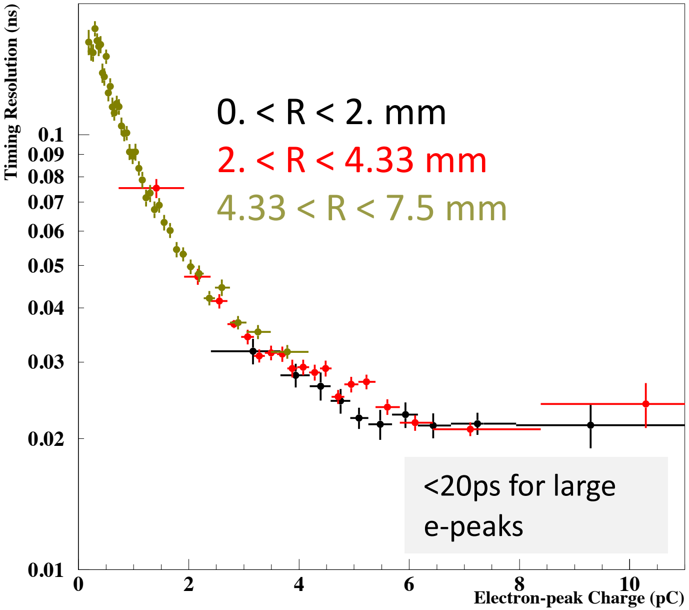

e-peak charge should have all info about where is Cherenkov cone compared to pad. Indeed, time resolution for each individual pad worsens as R increases!

Multi-pad MicroMegas – Individual pad response

Multi-pad: Same resolution as single-pad

At center of each pad (0<R<2mm):

Timing resolution of **25ps for all pads**

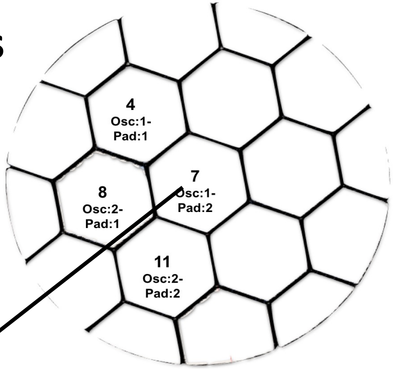

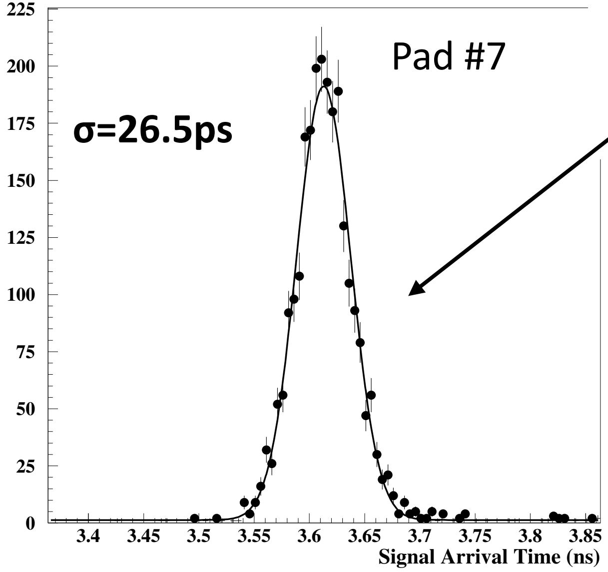

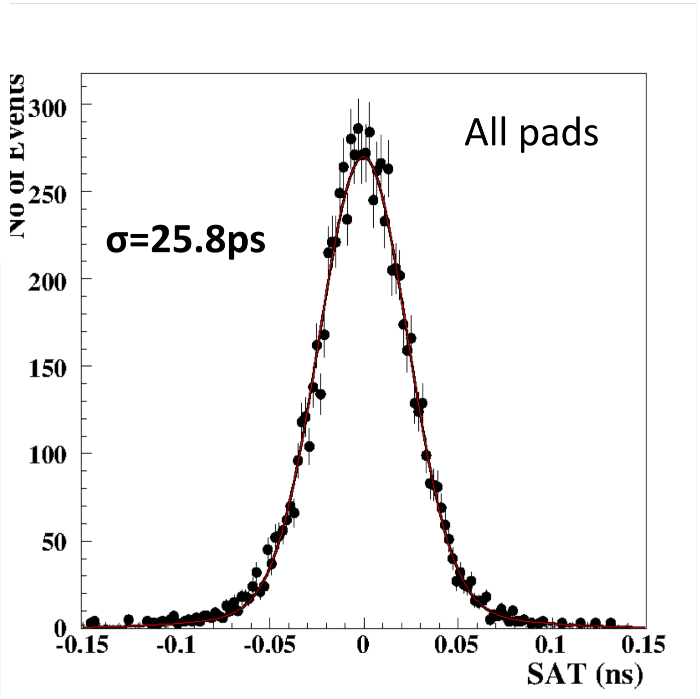

Multi-pad MicroMegas – The "3 pads" region

Not the easiest regions

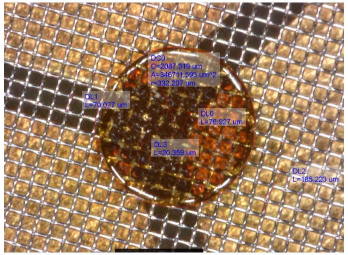

Pillars of ~650µm diameter

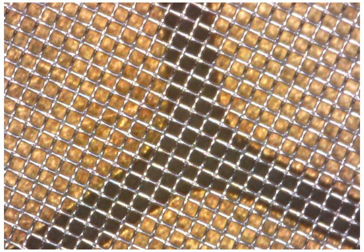

200µm inter-pad space

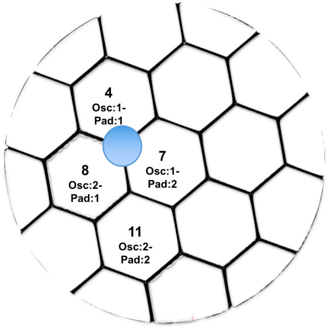

Individual pad responses

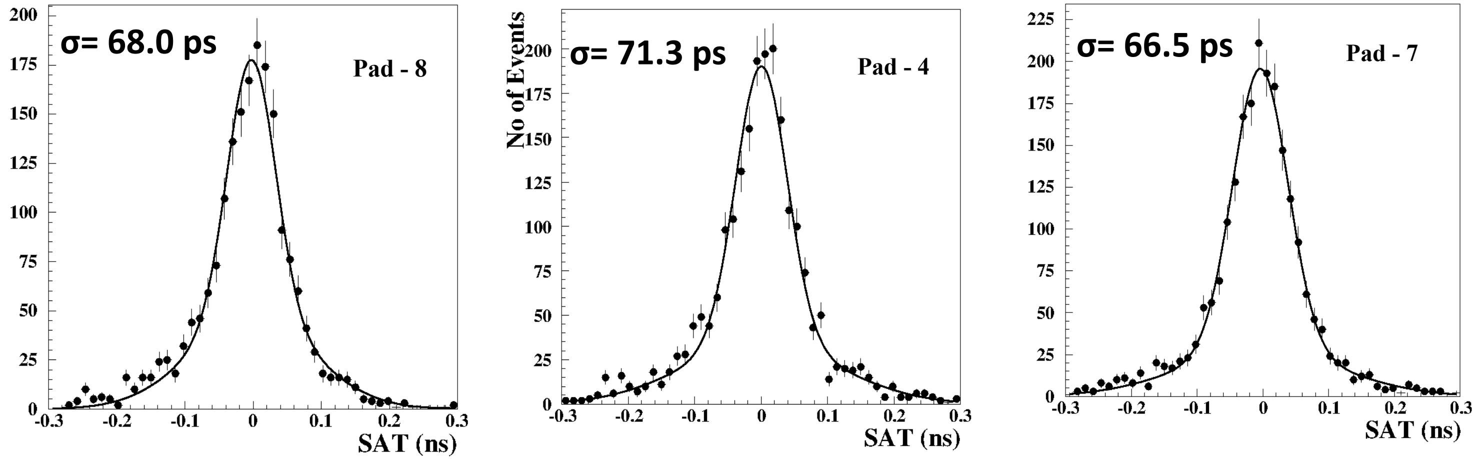

SAT: Signal Arrival Time

Naive estimation:
<σ>/sqrt(3)≈**40 ps**

Multi-pad MicroMegas – The "3 pads" region

combined pad response

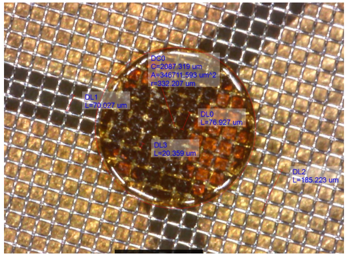

Pillars of ~650µm diameter

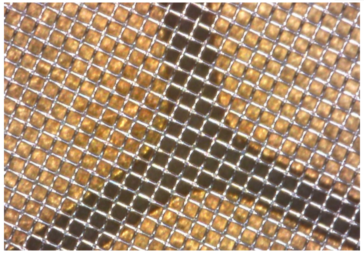

200µm inter-pad space

$$\chi^2 = \sum_{m=1,M} \frac{\left(T_{comb.} - \left[T^m_{f-corr.} - \tau\left(Q^m_e\right)\right]\right)^2}{\sigma^2\left(Q^m_e\right)}$$

$$\hat{T}_{comb.} = \frac{\sum\limits_{m=1,M} \frac{\left(T^m_{f-corr.} - \tau\left(Q^m_e\right)\right)^2}{\sigma^2\left(Q^m_e\right)}}{\sum\limits_{m=1,M} \frac{1}{\sigma^2\left(Q^m_e\right)}}$$

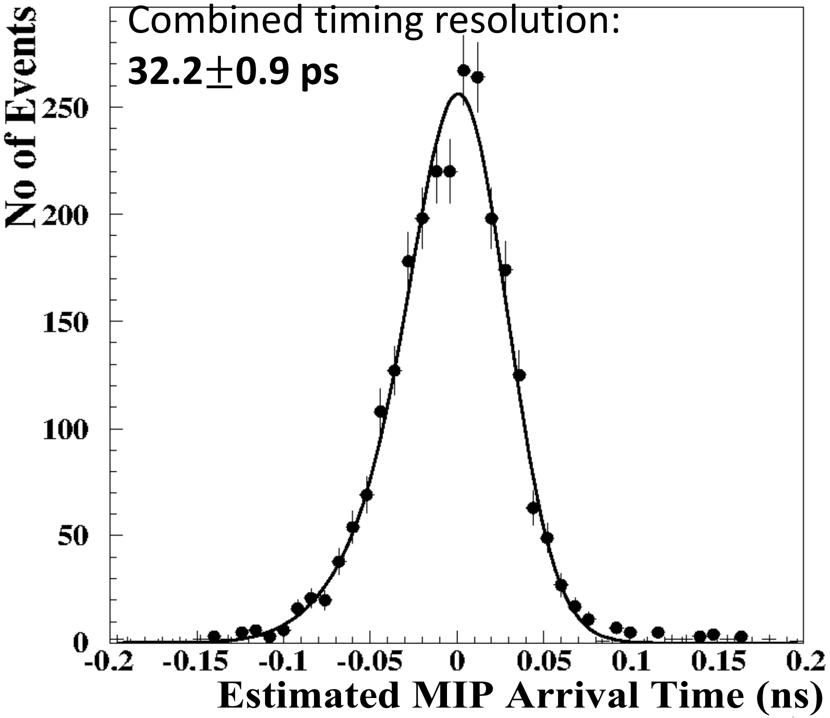

S. Aune et al. for the PICOSEC Collaboration, NIM-A, Vol. 993, (2021), 165076 - arXiv:2012.00545v2

Summary – Outlook

Coupling a Micromegas detector with a radiator / photocathode we have **surpassed the physical constrains on precise timing with MPGDs**, achieving two orders of magnitude improvement:

- **σ_t~ 76 ps for single p.e.**
- **σ_t~ 24 ps**(with the "standard" setup)for 150 GeV muons with 3 mm MgF_2 + 5.5 nm Cr substrate + 18 nm CsI photocathode,**$\langle N_{p.e.} \rangle \approx 10$**
- Almost same timing resolution for multi-pad

PICOSEC Micromegas is a well-understood detector

- reproduce observed behavior with detailed simulations and a phenomenological model: valuable tool for parameter-space exploration

Summary – Outlook

Towards a large-scale detector, following steps for the near future:

- Commission & test the new, modular prototype with Micromegas on a ceramic PCB
- Utilize the experience from ATLAS NSW Micromegas to produce flat large area detectors
- Test DLC & B4C photocathodes on MIP beams to address Q.E. and robustness
- Investigate GaN potential for high efficiency photocathodes
- Upgrade to electronics for data acquisition (SAMPIC digitizer)
- Address the concept of the PICOSEC Micromegas embedded in an EMC. Test in electron beams.

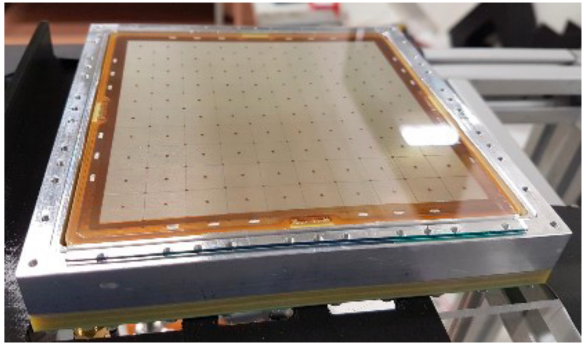

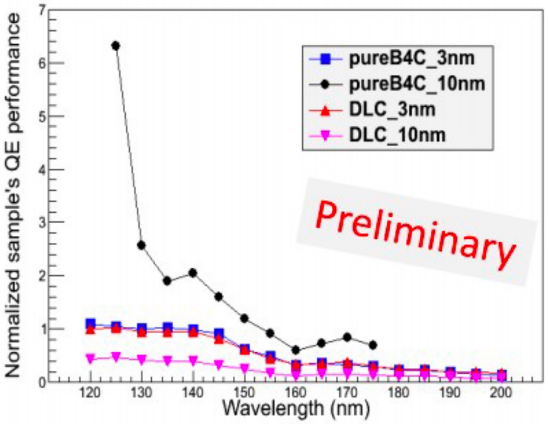

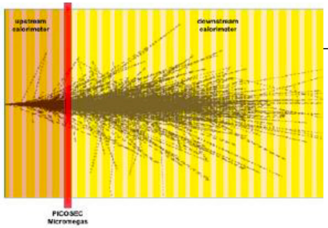

Data from laser test with ~70 p.e.

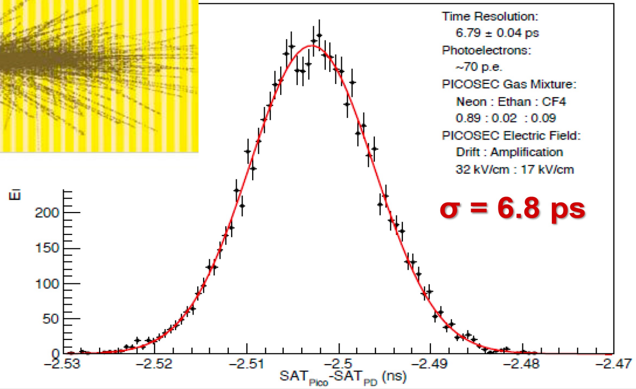

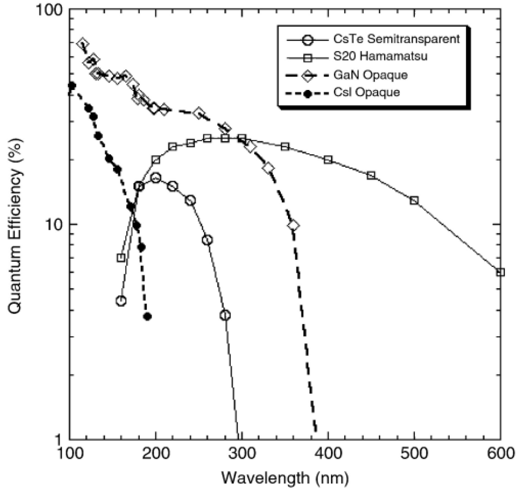

Thank you

Signal processing (1)

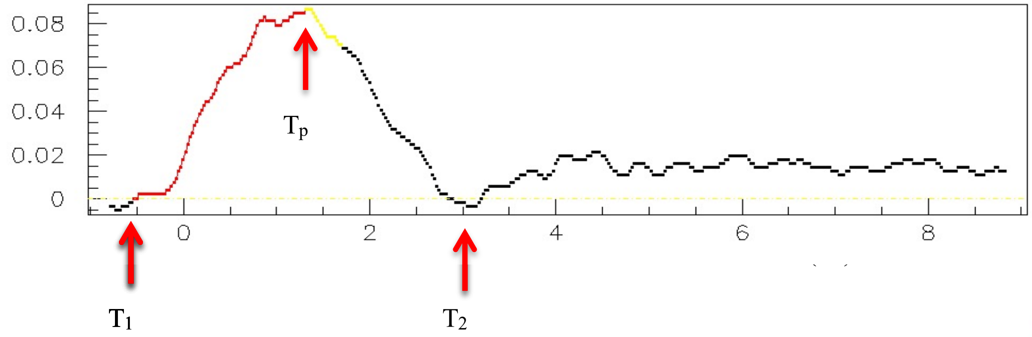

- Recognize the “start”, “peak” and “end” of the e-peak
- Evaluate charge by integrating the relevant part
- Fit the e-peak pulse in order to neutralize noise effects using the difference of two logistic functions

$$f(t;p_0,p_1,p_2,p_3,p_4,p_5,p_6) = \frac{p_0}{\left(1+e^{-(t-p_1)p_2}\right)^{p_3}} - \frac{p_0}{\left(1+e^{-(t-p_4)p_5}\right)^{p_6}}$$

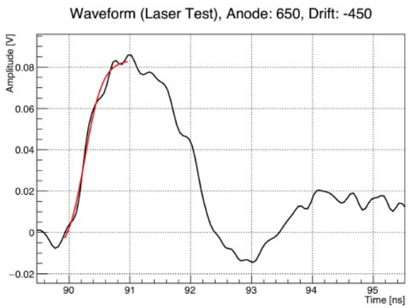

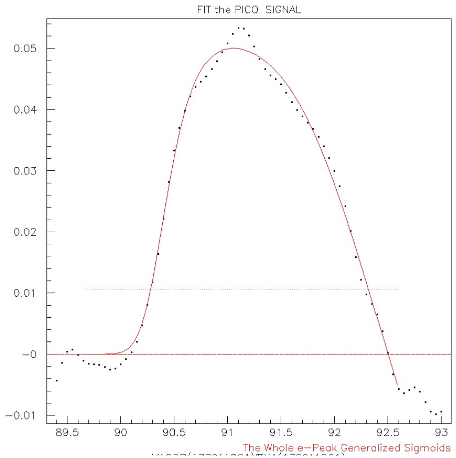

Fit with the fifference of two logistic functioonsare used to define the “**start**” and ”**end**” points of the e-peak waveform, to estimate **charge** and it is also used for **timing**

Stage 3 – Electronics (2) – technique is consistent and unibiased

See RD51 Notes 2017-011
And 2018-004 (Kostas Paraschou's thesis)

$\bar{S}(t)$

$$P_{Q_{tot}=Q}(\tau_1, ..., \tau_k, q_1, ..., q_k; k) =$$

$$= \frac{\delta\left(Q - \sum_{i=1}^{k} q_i\right) \cdot R(k) \cdot \prod_{i=1}^{k} \Phi(\tau_i; k) \cdot \prod_{i=1}^{k} G(q_i)}{N(k)}$$

where

$$N(k) = \int_0^\infty \cdots \int_0^\infty \delta\left(Q - \sum_{i=1}^{k} q_i\right) \cdot R(k) \cdot \prod_{i=1}^{k} G(q_i) dq_1 ... dq_k$$

$$\langle S(t) \rangle_{Q_{tot}=Q} =$$

$$= \sum_{k=1}^{\infty} R(k) \int_0^\infty \cdots \int_0^\infty \sum_{i=1}^{k} q_i f(t - \tau_i) \cdot \delta\left(Q - \sum_{i=1}^{k} q_i\right) \cdot$$

$$\cdot \prod_{j=1}^{k} \Phi(\tau_j; k) \cdot \prod_{j=1}^{k} G(q_j) dq_1 ... dq_k d\tau_1 ... d\tau_k$$

$$\langle S(t) \rangle_{Q_{tot}=Q} = \sum_{k=1}^{\infty} R(k) \sum_{i=1}^{k} \int_0^\infty f(t - \tau_i) \Phi(\tau_i; k) d\tau_i \cdot$$

$$\cdot \int_0^\infty \cdots \int_0^\infty q_i \cdot \delta\left(Q - \sum_{i=1}^{k} q_i\right) \cdot \prod_{j=1}^{k} G(q_i) dq_1 ... dq_k$$

$$\langle q_i \rangle_{Q=\sum_{j=1}^{k} q_j} = \frac{\int_0^\infty \cdots \int_0^\infty q_i \cdot \delta\left(Q - \sum_{i=1}^{k} q_i\right) \cdot \prod_{j=1}^{k} G(q_i) dq_1 ... dq_k}{N(k)}$$

$$\langle S(t) \rangle_{Q_{tot}=Q} = \sum_{k=1}^{\infty} R(k) N(k) \sum_{i=1}^{k} \int_0^\infty f(t - \tau_i) \Phi(\tau_i; k) d\tau_i \cdot$$

$$\cdot \int_0^\infty \cdots \int_0^\infty \frac{q_i \cdot \delta\left(Q - \sum_{i=1}^{k} q_i\right) \cdot \prod_{j=1}^{k} G(q_i)}{N(k)} dq_1 ... dq_k$$

$$\langle S(t) \rangle_{Q_{tot}=Q} = \sum_{k=1}^{\infty} R(k) N(k) \cdot \sum_{i=1}^{k} \langle q_i \rangle_{Q=\sum_{j=1}^{k} q_j} \int_0^\infty f(t - \tau_i) \Phi(\tau_i; k) d\tau_i$$

$$\int_0^\infty f(t - \tau_i) \Phi(\tau_i; k) d\tau_i = \int_0^\infty f(t - \tau) \Phi(\tau; k) d\tau$$

$$\langle S(t) \rangle_{Q_{tot}=Q} = \sum_{k=1}^{\infty} R(k) N(k) \int_0^\infty f(t - \tau) \Phi(\tau; k) d\tau \sum_{i=1}^{k} \langle q_i \rangle_{Q=\sum_{j=1}^{k} q_j}$$

$$= Q \sum_{k=1}^{\infty} R(k) N(k) \int_0^\infty f(t - \tau) \Phi(\tau; k) d\tau$$

$$= Q \int_0^\infty f(t - \tau) \left\{ \sum_{k=1}^{\infty} R(k) N(k) \Phi(\tau; k) \right\} d\tau$$

$$\langle \Phi(\tau) \rangle_{Q_{tot}=Q} = \sum_{k=1}^{\infty} R(k) N(k) \Phi(\tau; k)$$

Understood in terms of phenomenological model

- Known in literature that quenchers in the gas-mix increase drift velocity →
- **Model**: assume a time-gain per inelastic interaction compared to elastic interactions

Time spread (ns) →

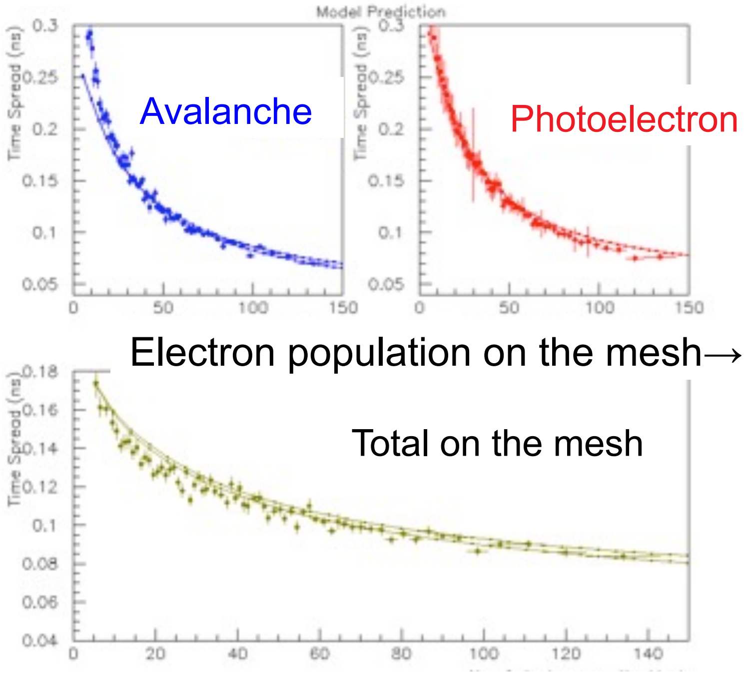

Electron polulation on the mesh→

Time (ns)

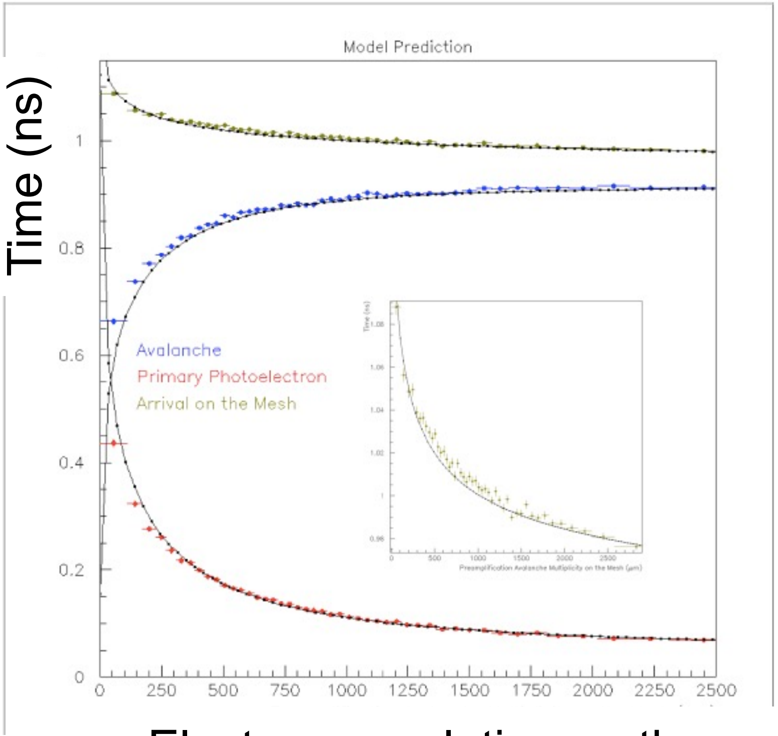

Electron population on the mesh

arXiv:1901.10779v1 [physics.ins-det]

Detector stability – Resistive Micromegas

Best resolution was at voltages which give high currents on anode: **robust anode**

Resistive strips (MAMMA)

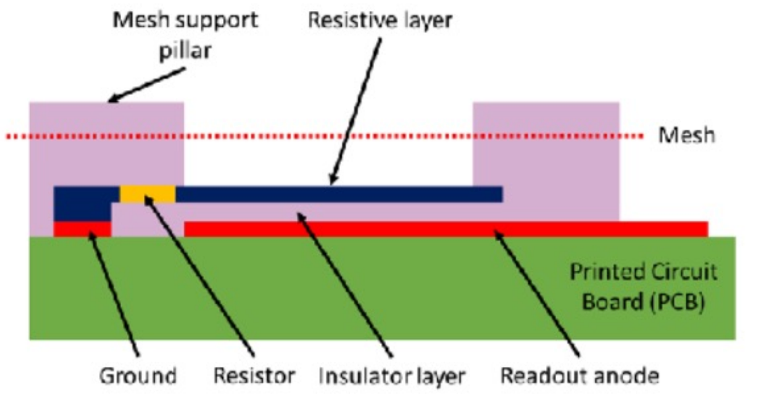

Readout beneath resistive layer: picks up signal from above

Floating strips (COMPASS)

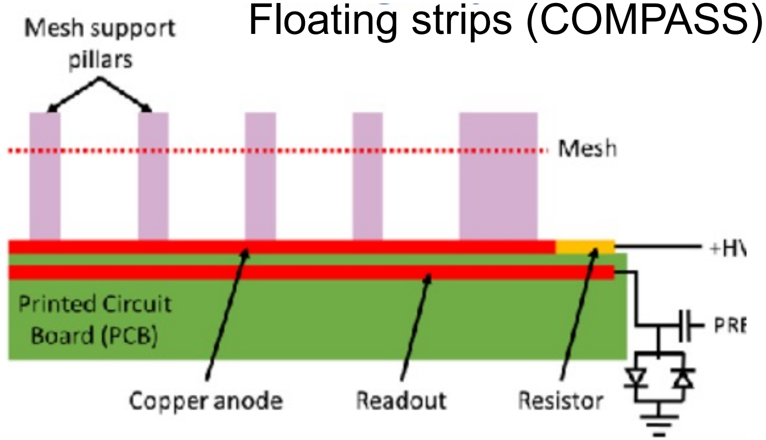

Copper Layer to HV via resistor; Readout "floating"

Non resistive ← MAMMA results → With resistive strip

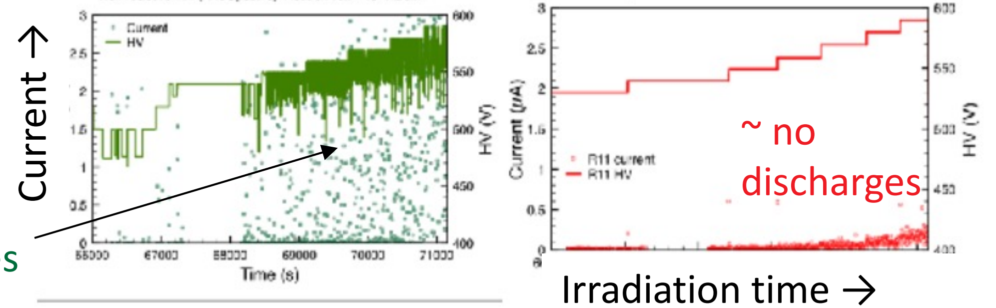

discharges

Resistive readouts operate stably at high gain in neutron fluxes of 10^6 Hz/cm^2.

T. Alexopoulos *et al.*, *NIMA* **640** (2011) 110-118.

GaN:

- Higher quantum efficiency than CsI
- Broader bandwidth towards higher wavelengths ➔ Quartz instead of MgF_2 ?
- Aging & Stability in the gas?
  → A GaN sputtering target just received!

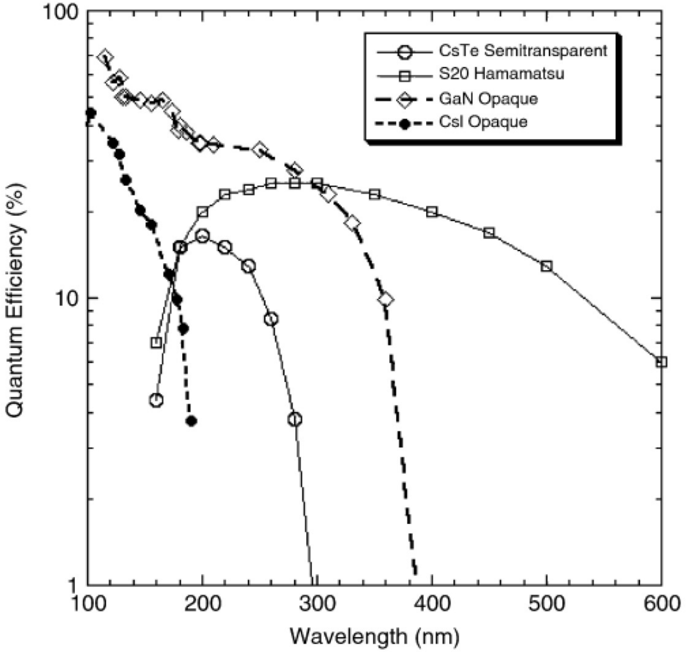

O. Siegmund, et al, "Development of GaN photocathodes for UV detectors" *Nucl. Instr. and Meth. A,* vol. 567, 1, 89-92, 2006, https://doi.org/10.1016/j.nima.2006.05.117

Embed a PICOSEC-Micromegas layer inside an electromagnetic calorimeter after few radiation lengths

- From some simple simulations: a 30 GeV electron produces **~200 p.e.** in MgF2 with a metallic (**Cr**) photocathode after **2 radiation lengths**
- **Time resolution < 10 ns !!**
- No need for high efficiency photocathode
- No need for extremely high electric fields
- To be tested at SPS in 2021

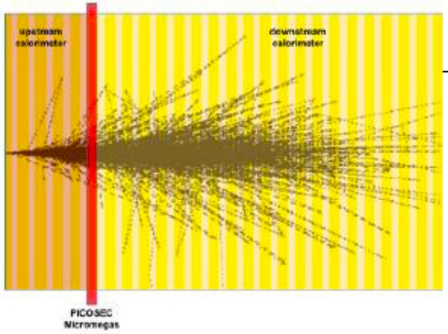

Data from laser test with ~70 p.e.